ADDIS ABABA UNIVERSITY

ADDIS ABABA INSTITUTE OF TECHNOLOGY

SCHOOL OF CIVIL AND ENVIRONMENTAL ENGINEERING

PARAMETRIC STUDY ON THE USE OF ADDITIONAL STEEL PLATES FOR CONFINEMENT OF AXIALLY LOADED REINFORCED CONCRETE COLUMNS

A Thesis in Structural Engineering

By: Kassahun Tilahun

December, 2023

Addis Ababa

A Thesis

Submitted in Partial Fulfillment of the Requirements for the Degree of Master of Science

The undersigned have examined the thesis entitled **'Parametric Study on the Use of Additional Steel Plates for Confinement of Axially Loaded Reinforced Concrete Columns'** presented by **Kassahun Tilahun**, a candidate for the degree of **Master of Science** and hereby certify that it is worthy of acceptance.

Dr.- Ing.Adil Zekaria		29/12/2023
Advisor	Signature	Date
Dr. Abrham Gebre		26/12/2023
Internal Examiner	Signature	Date
Dr.- Ing. Bedilu Habte		Dec. 26/2023
External Examiner	Signature	Date
Chair person	Signature	Date

Abrham Gebre (Dr.)
Dean, School of Civil & Environmental Engineering

Addis Ababa University
Addis Abeba Institute of Technology
Director of Postgraduate Program

UNDERTAKING

I certify that research work titled **"Parametric Study on the Use of Additional Steel Plates for Confinement of Axially Loaded Reinforced Concrete Columns"** is my own work. The work has not been presented elsewhere for assessment. Where material has been used from other sources it has been properly acknowledged / referred.

Name: - Kassahun Tilahun

Signature: - 

Date: - December, 2023

ABSTRACT

Ductility is the ability of a structure or its components to offer resistance in the inelastic domain of response. However, concrete is not a ductile material, and therefore, confinement is recommended to improve its performance. Confinement in concrete is achieved by the suitable placement of transverse reinforcement, which results in a significant increase in the strength and ductility of concrete. This paper focuses on the confinement effect induced by different arrangements of transverse reinforcement on axially loaded concrete columns. The aim of this research is to carry out a parametric study on the confinement action induced by a type of stirrup involving steel plates and different arrangements of transverse reinforcement on axially loaded concrete columns. To achieve this goal, numerical analysis was conducted using the finite element program, ABAQUS. The variables considered in this study were concrete compressive strength, spacing of transverse reinforcement, arrangement of transverse reinforcement, and influence of plate thickness. The results of numerical studies have shown that the effect of concrete compressive strength and longitudinal reinforcement ratio have the most impact on the column response, the spacing of transverse reinforcement has less impact and the effect of plate thickness almost negligible. Additionally, the configuration of transverse reinforcement involving steel plates has been found to improve a column's strength and its ability to withstand axial loads.

Key Words: Parametric study, steel plates, axially loaded, confinement effect, stirrups.

ACKNOWLEDGMENTS

First of all, I praise and thank Almighty God for giving me the strength and ability to complete this research work.

I would like to express my sincere appreciation, respect, and profound gratitude to my advisor, Dr. Ing.Adil Zekaria, for his invaluable guidance, endless support, and constant encouragement throughout the overall path of this research. During the course of my master's study, his invaluable ideas, guidance, and trust helped me overcome a number of difficulties arising in this research. I am very grateful to have had the opportunity to learn so many notions and concepts from him during the course of this research; without him, this research would not have been possible. I would also like to thank him for all I have learned from him; his insights and professional opinions pushed me towards new limits.

Afterwards, I would like to thank Dr. Abrham Gebre for his kindly help, encouragement, and constructive ideas during the course of this research.

I am grateful to many of my friends and to all individuals who have contributed directly or indirectly to providing a stimulating environment throughout the course of this thesis.

Last but not least, I would like to thank my mother, my sister, and my brother for their constant encouragement and tremendous support.

TABLE OF CONTENTS

LIST OF TABLES

LIST OF FIGURES

LIST OF ABBRIVIATIONS AND SYMBOLS

ρ_{cc} = Area ratio of total longitudinal steel to concrete core

ρ_s = Volumetric ratio of transverse reinforcement

A_g =Gross area of concrete section

f'_c = unconfined cylindrical strength of concrete

f_{co} = Unconfined concrete compressive strength

f'_l = Effective transverse confining pressure

k_e = Confinement efficiency coefficient

f_y = Yield strength of longitudinal reinforcing steel

f_{yh} = Yield strength of transverse reinforcing steel

ε_t^{pl} = Tensile equivalent plastic strain

ε_c^{pl} = Compressive equivalent plastic strain in

ε_c^{in} = Compressive inelastic strain

ε_{cr} = Crack strain

ε_{oc}^{el} = Elastic strain

d_c = Compressive damage parameter

d_t = Tensile damage parameter

Es = Modulus of elasticity for steel

Ec = Modulus of elasticity for concrete

f_y = Yield stress of steel

f_u = Ultimate stress of steel

σ_t = Tensile stress

σ_c = Compressive stress

ε_t = Total tensile strain

ε_c = Total compressive strain

ε_u = Ultimate strain

ε_y = Yield strain

ν = Poison's ratio

ψ = Dilation angle

σ_{bo}/σ_{co} = Ratio of biaxial to uniaxial compressive strength

Kc = Second stress invariant ratio

e =Eccentricity value in ABAQUS

s = vertical spacing of transverse reinforcement

N* = Axial compressive load on column

φ = Strength reduction factor

RC = Reinforced concrete

CDP = Concrete damage plasticity

FEM = Finite element method

FE = Finite element

CHAPTER 1 INTRODUCTION

1.1 Background

The primary structural members that are primarily subject to axial forces with or without moment are columns. The collapse of a column causes the entire structure to buckle under axial load and expand laterally. By confining the core concrete with transverse reinforcement, a process known as confinement, it is possible to prevent excessive lateral expansion and stiffness deterioration. Concrete is typically constrained when it expands under axial loads by steel spirals or circular hoops that effectively restrain and counteract this expansion. other common transverse reinforcement arrangements use square or rectangular hoops that can be strengthened even more by adding more cross-ties (or overlapping hoops) [1].

Sheikh [2] demonstrated that columns' strength and ductility could be increased by placing longitudinal reinforcement bars around the perimeter of the core and confining these bars with laterals like ties. As a result, RC columns need to be reinforced both longitudinally and laterally. Hoop stress is applied to the confining volume while the concrete core is compressed radially in the horizontal direction. On the other hand, either the wide or the close spacing between ties is what prevents the concrete core from being confined high volumetric ratio of ties damages concrete continuity and creates a weak plane between the core and the concrete cover, in addition to complicating construction due to the congested column cage with reinforcement [3, 4]. Welded reinforcement grids were used by Saatcioglu and Grira [5] and Ksuma et al. [6] to reduce reinforcement congestion due to overlapping hoops, bends, and bend extensions.

It is well known that by confining the column's core, lateral reinforcement significantly improves the strength and ductility of reinforced concrete columns. Confinement increases the concrete core's ability to withstand significant deformations without suffering a significant loss in strength, while reducing the loss of strength caused by the concrete cover collapsing. For reinforced concrete building columns, the confinement-induced increase in capacity, particularly in ductile behavior, is essential. The arrangement, size, longitudinal reinforcement, transverse reinforcement spacing, and confining methods all have a direct impact on the degree of confinement.

Due to the lack of confinement offered by ties, additional steel plates were used to further restrain the concrete core. Steel spirals or circular hoops are typically used as confinement to limit and effectively contrast the expansion of concrete under axial loads. Another commonly used configuration for lateral reinforcement is square or rectangular ties, which can be made even stronger by including more cross-ties. The latter are crucial in limiting the distance between successive transverse sets, increasing the size of the effectively confined concrete area.

This study focuses on the confinement effect resulting from various configurations of transverse reinforcement on axially loaded columns. A parametric study will be carried out, comprising different concrete columns with different mechanical strengths and reinforced with three different layouts of stirrups, namely closed square hoops, closed stirrups with additional cross ties, and a type of stirrup involving additional restraint plates.

1.2 Statement of the Problem

The confined concrete act as a two-phase material when subjected to axial load: one phase is that related to the area inside the stirrups, which is the effectively confined core, and the other phase is represented by the concrete cover beyond the stirrups' perimeter, which is unconfined. While tested in compression, the stirrups keep the internal concrete core from expanding laterally. To maximize the effectively confined concrete core one could reduce the stirrups spacing along the height of the column or introduce additional cross ties to limit the free span of the stirrups. Building on this concept, a type of stirrup involving additional restraint plates, has been designed that is able to extend the effectiveness of the confinement action applied by the stirrups over a wider area. The motivation of this type of reinforcement scheme is to obtain an enhanced diffused confinement action in order to limit spalling of the cover concrete under axial load.

1.3 Objectives

1.3.1 General Objective

The objective of this study is to investigate the confinement effect induced by a stirrup with additional steel plates and different arrangements of transverse reinforcement on axially loaded concrete columns.

1.3.2 Specific Objective

This thesis has a specific objective of conducting parametric study: -

- ✓ Evaluating the effectiveness for section confined by a stirrup with additional steel plates in enhancing the confinement effect on the concrete column.
- ✓ Analyzing how different parameters such as concrete compressive strength, spacing of transverse reinforcement, longitudinal reinforcement ratio, arrangement of transverse reinforcement and influence of plate thickness, affect the concrete confinement behavior.
- ✓ Assessing the behavior of the concrete column, such as strength, ductility, and deformation capacity, under different confinement conditions.

1.4 Scope

This research paper's scope is limited to axially loaded reinforced concrete columns reinforced with three different layouts of stirrups: stirrup with additional cross ties, closed square hoops, or stirrups with additional restraint plates. Furthermore, the parameters investigated in this study were the compressive strength of concrete, longitudinal reinforcement ratio, spacing of transverse reinforcement, configuration of transverse reinforcement, and thickness of the plates.

1.5 Organization of the thesis

There are five chapters in this study. The introduction, problem statement, objectives, and study scope are all presented in the first chapter. Chapter two presents the previous research on the transverse reinforcement for concrete confinement. under this study, the literature review was described in two ways: (1) based on analytical modeling of confined concrete, and (2) experimental research on confined concrete. In the third chapter, the details of the work methodology include a description of the model specimen's geometry and reinforcement details, elements, boundary conditions, load application, meshing, and the solution method used to simulate an axially loaded reinforced concrete column. The fourth chapter uses Abaqus/CAE to present the finite element analysis of an axially loaded, confined concrete column. Abaqus' output results include load-displacement curves and stress-strain curves. Additionally, a thorough discussion of the nonlinear finite element model's verification using results from previously tested specimens is provided. The last chapter presents conclusions based on the findings of the current research and recommendations for future work.

CHAPTER 2 LITRATURE REVIEW

2.1 General

2.1.1 Confined Concrete

A reinforced concrete column experiences lateral expansion when an axial load is applied as a result of the Poisson's consequences. The transverse reinforcement in the column produces a confinement effect that restricts the lateral expansion of the concrete. This effect transforms the compression stress state of concrete from a uniaxial to a multiaxial stress state, this effect increasing the column's ability to resist loads and its ductility. Confined concrete generally fails in a ductile manner, whereas unconfined concrete fails in a brittle manner [7].

In reinforced concrete columns, there is an assumption that there will be an arching action among the levels of lateral reinforcement. The theory is that the arching action behaves as parabolas using an initial slope of 45° because it occurs both horizontally and vertically between restrained longitudinal bars [8].

The assumed arching action among the levels of lateral reinforcement is shown in Figures 2.1 and 2.2. Halfway between the levels of the transverse reinforcement, the area of ineffectively confined concrete will be the largest and the area of effectively confined concrete core will be the smallest [9].

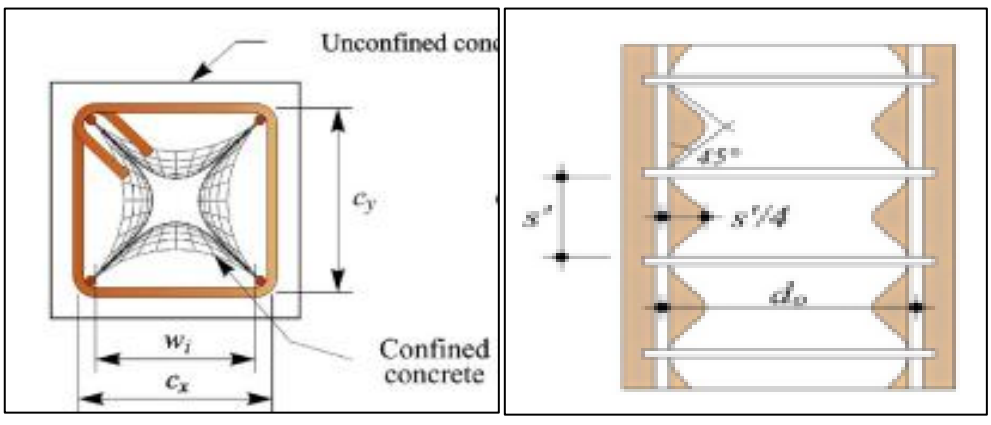

Figure 2. 1 Effectively-confined core for square concrete column elements

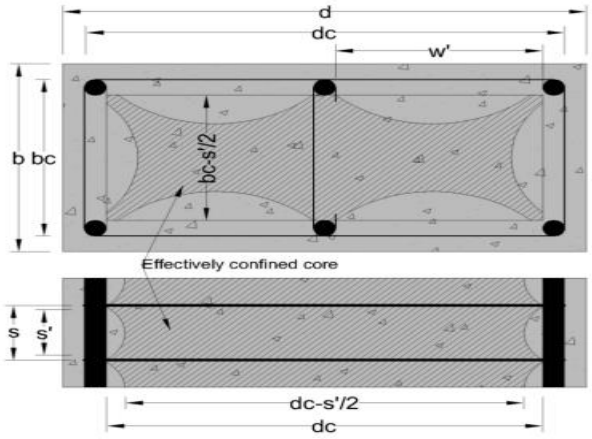

Figure 2. 2 Effectively-confined core for rectangular hoop.

2.1.2. Parameters affecting concrete confinement

a. The arrangement of transverse reinforcement:

The arrangement of transverse reinforcement in reinforced concrete columns is an important factor that affects the columns' capacity for lateral confinement. The strength and transverse reinforcement arrangement can influence the lateral confinement capacity of the columns.

b. The compressive strength of concrete:

The compressive strength of concrete is a parameter that can affect concrete confinement in a reinforced concrete column. High-strength concrete has a higher compressive strength, which means it can withstand higher loads and resist lateral forces more effectively. On the other hand, low-strength concrete may have lower compressive strength and may not provide sufficient confinement to the longitudinal bars [7].

c. Axial load level:

The axial load level is a parameter that can affect the confinement of concrete and the strength of a reinforced concrete column. A column that is imposed to an axial load, it experiences compressive forces that can cause the concrete to expand laterally. At low levels of axial load, the confinement offered by the reinforcement is generally sufficient to prevent excessive expansion to the side of the concrete. This allows that column to exhibit its full-strength potential and maintain its integrity. As the axial load rises, however, the concrete's expansion at the sides becomes more significant. This can lead to

a reduction in the effectiveness of the confinement provided by the reinforcement. As a result, the column may experience reduced strength and ductility [10].

d. Yield strength of transverse reinforcement (f_{yt})

Strength of transverse reinforcement at yield directly affects its ability to confine the concrete core effectively. If the yield strength of the lateral reinforcement is low, it may not be able to resist the lateral forces adequately, leading to a reduced confinement effect.

e. Spacing of transverse reinforcement

When the transverse reinforcement is spaced widely, it reduces the amount of confinement provided to the concrete. This may cause the concrete's expanding laterally under axial load to increase, causing the column's strength and ductility to reduced. The concrete's strength and ductility are increased by the smaller spacing, which helps to prevent lateral expansion of the material.

f. Volumetric ratio of lateral reinforcement (ρ_t)

The volumetric ratio (ρ_t) of the lateral reinforcement is directly correlated with the confining pressure exerted within the concrete column's core. By applying more lateral confining pressure to the concrete core, the confining impact will be enhanced. Therefore, the peak strength and toughness of concrete are proportionally related to the volumetric ratio of transverse steel [11].

g. longitudinal reinforcement ratio

The size and amount of longitudinal reinforcement enhance the effect confinement by preventing the lateral expansion of the core. The bars' contribution to confinement increases in direct proportion to their longitudinal reinforcement ratio and bar diameter [12].

For RC columns, the practical longitudinal reinforcement ratio ranges from 1% to 4% [13]. The following is the definition of the longitudinal reinforcement ratio:

$\rho = (A_s/A_g)$

2.1.3. Confinement action of lateral reinforcement

In reinforced concrete columns, the ability of transverse reinforcement to strengthen and contain the concrete core is referred to as having a confinement action. To improve the ductility and strength of the column, transverse reinforcement, such as stirrups or ties, is positioned all the way around its longitudinal bars. It serves as a cage, reducing the concrete's ability to expand and enhancing its resistance to compression. This confinement also helps in controlling cracking and improves the column's capacity to deform prior to failure, giving warning signs. The placement of the reinforcement affects the confinement's effectiveness and increases the column's capacity for carrying loads. To maintain constant deformation capacity, the confinement reinforcement should be increased as the axial load increases [14].

2.1.4. Mechanisms of concrete confinement

Concrete expands laterally under uniaxial compression, and the axial strains caused by this loading result in transverse tensile strains. This can result in vertical cracks and concrete failure. The concrete is confined by lateral pressure, which prevents lateral expansion and significantly increases ductility while also improve the strength.

Sheikh [2] explained that the core and the cover of a concrete member will react differently to an axial load when it is effectively confined. Because lateral expansion of concrete is small at low longitudinal strain levels, Transverse reinforcement has little effect on lateral confinement. But as longitudinal strains rise, concrete's lateral strains also rise. The transverse reinforcement prevents the concrete in the core from expanding, which keeps the core contained and separates the cover from the core. While the core concrete continues to sustain high strains of stress, the cover concrete behaves like unconfined concrete and loses effectiveness once it reaches compressive strength. The type of confinement will determine the concrete core's ability to support loads after the cover spalls. Therefore, the distributions of stress from compression for the cover layer and inner concrete, respectively, follow the constrained and unrestrained concrete stress-strain relations.

The arrangement of the lateral reinforcement affects how well confinement works. Spirals apply a different type of confinement pressure than do rectangular ties. Circular spirals exert a constant confining pressure on the core of concrete because of their shape, which is in axial hoop tension.

As a result, spirals or circular hoops effectively confined the concrete core. The restraining force generated in the hoop steel determines how evenly the confining pressure provided by ties is applied. Low restraining action occurs between the comers, when longitudinal reinforcement is supporting the hoop steel at angles, high restraining forces are developed. This is because the pressure from the lateral concrete expansion under axial compression causes the sides of the ties to bend outward, because of their lack of stiffness, which causes reactive pressures to build up more intensely at the corners than they would elsewhere [15]. See Figure 2.3.

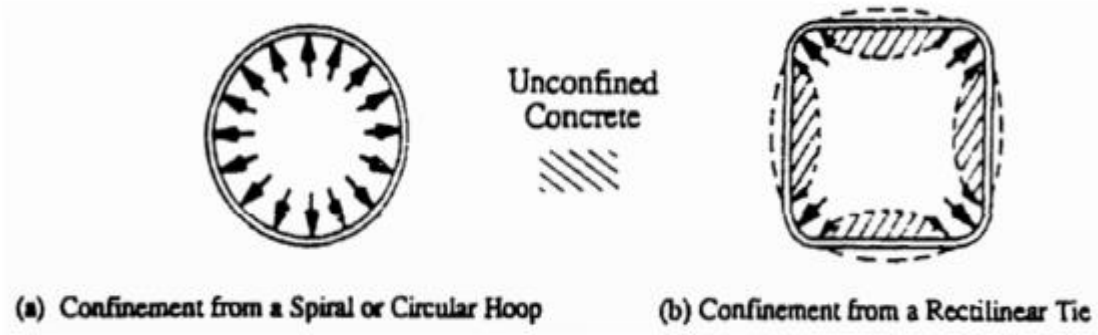

Figure 2. 3 Confinement from Transverse Reinforcement [15]

2.2 Research on analytical modeling of confined concrete

Based on experimental results, a number of analytical models have been created to predict the stress-strain curve for laterally confined concrete.

Kent and Park [16] have presented a stress strain model of confined concrete for rectangular sections. The model was examined in light of earlier experimental results from Roy and Sozen [17] and Soliman and Yu [18]. Figure 2.4 shows the stress-strain curve developed by Kent and Park for concrete constrained by rectangular hoops. The proposed curve's ascending portion is represented by a second order parabola equation and is unaffected by confinement. The slope of the descending portion of the curve is expressed as a function of the volumetric ratio of the confining steel, the width of the confined core, the spacing between the hoops, and the cylindrical strength of the concrete.

Ascending part $f_c = f'_c \left(\frac{2\varepsilon_c}{\varepsilon_o} - \left(\frac{\varepsilon_c}{\varepsilon_o}\right)^2\right)$ 2.1

Where: f'_c is unconfined cylindrical strength of concrete ε_o is the corresponding strain

The formula for the stress-strain relationship's falling branch is given by

Descending part $f_c = f_c'(1 - Z(\varepsilon_c - \varepsilon_o))$ 2.2

In which $Z = \frac{0.5}{\varepsilon_{50h} + \varepsilon_{50u} - \varepsilon_o}$ 2.3

Where $\varepsilon_{50h} = \varepsilon_{50c} - \varepsilon_{50u}$

$\varepsilon_{50u} = \frac{3+0.29f_c'}{145f_c'-1000}$ $f_c'(in\ Mpa)$ 2.4

$\varepsilon_{50c} = \frac{3}{4}\rho_s\sqrt{\frac{h''}{s_h}}$ 2.5

Where the strains for confined and unconfined concrete, respectively, that correspond to the stress equal to 50% of the maximum concrete strength are denoted by ε_{50c} *and* ε_{50u}

ρ_s = volumetric ratio of confining steel,

h'' = the width of the confined core and s_h= spacing of the hops

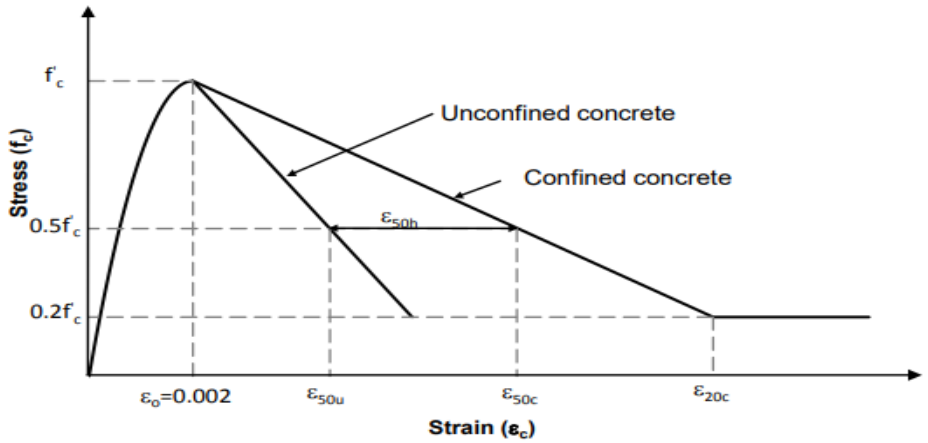

Figure 2. 4 Stress-Strain curve for Confined and unconfined Concrete [16].

Scott [19] investigation focused on several square solid columns that were transversely reinforced with overlapping hoop sets and either 8 or 12 longitudinal rebars. They used rapid strain rates in their tests, which are typical of seismic loading. When compared to the [16] model, which was verified against small-sized tests, the presence of good confining reinforcement details resulted in a significant increase in strength. As a result, simple modifications were made to the [16] model to include expansion in the compressive strength of confined concrete under high strain rates. The strain at significant concrete stress is 0.002K, and the excessive concrete stress is thought to be Kf'_c , where 'K' is a factor that is characterized later. Figure 2.5 depicts the Scott stress-strain curve for concrete constrained by rectangular hoops, and the equation express as:

For $\varepsilon_c \leq 0.002K$ $\quad f_c = Kf'_c \left(\frac{2\varepsilon_c}{0.002K} - \left(\frac{\varepsilon_c}{0.002K}\right)^2\right)$ 2.6

For $\varepsilon_c > 0.002K$ $\quad f_c = Kf'_c(1- Z_m(\varepsilon_c - 0.002K))$ 2.7

But not less than $0.2Kf'_c$

In which: $Z_m = \frac{0.5}{\frac{3+0.29f'_c}{145f'_c-1000}+\frac{3}{4}\rho_s\sqrt{\frac{h''}{s_h}}-0.002K}$ 2.8

Where: f'_c is in MPa, ρs = ratio of volume of rectangular steel hoops to volume of concrete core to the outside of the peripheral hoops, h " = width of concrete core to the outside of peripheral hoop and s_h= center to center spacing of hoops sets.

In the above expressions the value of 'K' is obtained from the expression:

$K = 1 + \frac{\rho_s f_{yh}}{f'_c}$ 2.9

Where: f_{yh} is the yield strength of the hoop reinforcement and the other parameters are as previously stated.

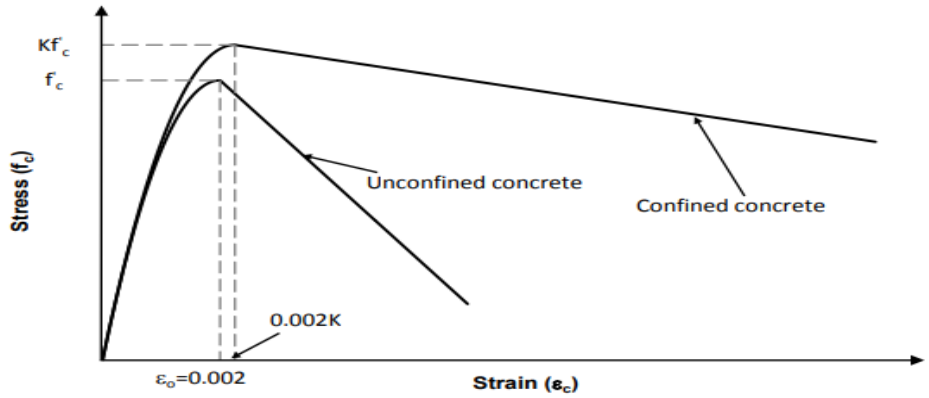

Figure 2. 5 Stress-Strain curve for Confined Concrete – Modified [19].

Mander [9] developed a unified stress-strain model for confined concrete that considers the effects of various forms of confinement by introducing an effective lateral confining pressure that works depending on how the lateral and longitudinal reinforcement are arranged. The model was expressed on the basis of the equation proposed by [20]. Figure 2.6 depicts the Mander stress-strain curve for concrete constrained by rectangular hoops. The confined concrete compressive strength $f'_{cc}$is calculated using the "five-parameter" multiaxial failure region mentioned by [21].

$$f_c = \frac{f'_{cc}\, xr}{r-1+x^r} \qquad 2.10$$

$$f'_{cc} = f'_c(-1.254 + 2.254\sqrt{1 + \frac{7.94f'_l}{f'_c}} - 2\frac{f'_l}{f'_c}) \qquad 2.11$$

In which f'_l is given by

$$f'_l = \frac{1}{2}k_e\rho_s f_{yh} \qquad 2.12$$

Where: ρ_s = ratio of volume of transverse confining steel to volume of confined concrete core,

f_{yh} = yield strength of transverse reinforcement, k_e= confinement coefficient.

for circular hoops $$k_e = \frac{\left(1-\frac{s'}{2d_s}\right)^2}{1-\rho_{cc}} \qquad 2.13$$

for circular spirals $$k_e = \frac{1-\frac{s'}{2d_s}}{1-\rho_{cc}}$$ 2.14

for rectangular section $$k_e = \frac{\left(1-\sum_{i=1}^{n}\frac{(w_i)^2}{6b_c d_c}\right)\left(1-\frac{s'}{2b_c}\right)\left(1-\frac{s'}{2d_c}\right)}{(1-\rho_{cc})}$$ 2.15

Where: ρ_{cc} = ratio of area of longitudinal reinforcement to area of core of the section, s' = clear spacing between transverse confining steels, d_s = diameter of spiral, d_c = core dimensions in x and y directions to centerlines of perimeter hoop, respectively, where $b_c > d_c$, s = center to center spacing transverse confining steels and w_i = distance between adjacent longitudinal steel in rectangular cross section.

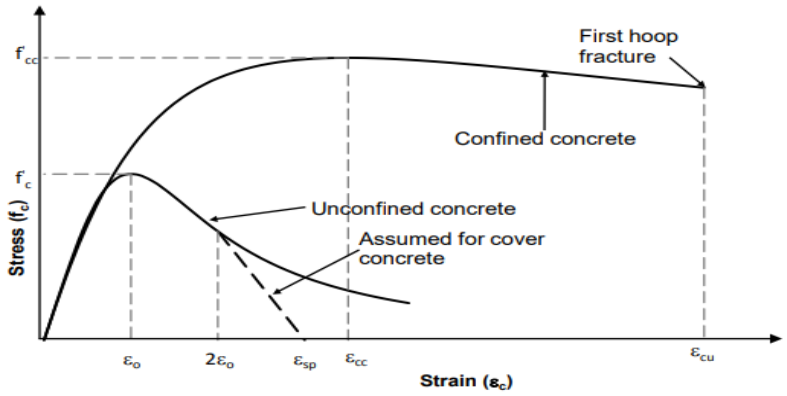

Figure 2. 6 Stress-Strain curve for Confined Concrete by Mander et al. [9].

According to Li et al.'s test analysis on circular and square RC columns [22], evaluated the performance of high-strength concrete columns constrained by conventional and transverse reinforcement with high yield strength and with various confinement proportions and arrangements was evaluated. According to their findings from the experiments, the confining reinforcement's yield strength and volumetric proportion. have a fundamental impact on how the stress strain curve behaves. Li [22] proposed a three-branch stress strain model for high strength concrete confined by either regular or high-yield strength transverse reinforcement, as shown in figure 2.7 and the equations expressed as:

$0 < \varepsilon_c \leq \varepsilon_{co}$ $$f_{c} = E_c\varepsilon_c + \left(\frac{f'_c - E_c\varepsilon_{co}}{\varepsilon_{co}^2}\right)\varepsilon_c^2$$ 2.16

$\varepsilon_{co} < \varepsilon_c < \varepsilon_{cc}$ $$f_{c} = f'_{cc} - \frac{(f'_{cc} - f'_c)}{(\varepsilon_{cc} - \varepsilon_{co})^2}(\varepsilon_c - \varepsilon_{co})^2$$ 2.17

$\varepsilon_c > \varepsilon_{cc}$ $$f_c = f'_{cc} - \beta \frac{f'_{cc}}{\varepsilon_{cc}} (\varepsilon_c - \varepsilon_{cc}) > 0.4 f'_{cc}$$ 2.18

In which, the maximum confined concrete compressive strength is given by

$$f'_{cc} = f'_c \left(-1.254 + 2.254 \sqrt{1 + \frac{7.94 f'_l}{f'_c}} - 2\alpha_s \frac{f'_l}{f'_c}\right)$$ 2.19

When $f'_c \leq 52Mpa$ $$\alpha_s = (21.2 - 0.35 f'_c)\frac{f'_l}{f'_c}$$ 2.20

When $f'_c > 52$Mpa $$\alpha_s = 3.1 \frac{f'_l}{f'_c}$$ 2.21

The parameter β controls the stress-strain model's post-peak branch's slope. where f'_l is the effective lateral confining pressure, calculated using the equations proposed by [9].

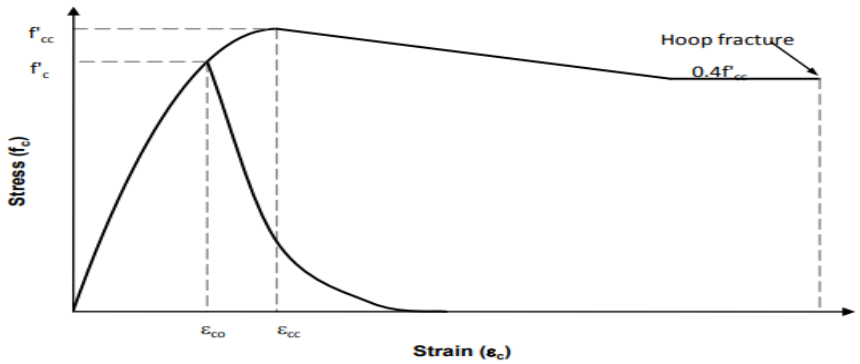

Figure 2. 7 Stress-Strain curve for Confined Concrete Proposed by Li et al. [22].

2.3 Research on experimental program of confined concrete

Dario [23] experimentally investigated the confinement influence of various configuration of lateral reinforcement on axially loaded concrete columns until failure. In an experiment, eighteen concrete columns with various arrangement of transvers reinforcement were tested. The columns were reinforced with: regular tie, stirrups with a cross ties, and a stirrup with additional restraint plates. Using ordinary Portland cement and aggregates, two different batches of concrete were used: compressive strength of concrete about 10 MPa was used to construct nine columns, and compressive strength of concrete about 30 MPa was used to construct the remaining nine columns. Each of the tested columns has a 25 x 25 cm square cross-section, and height of 40cm.

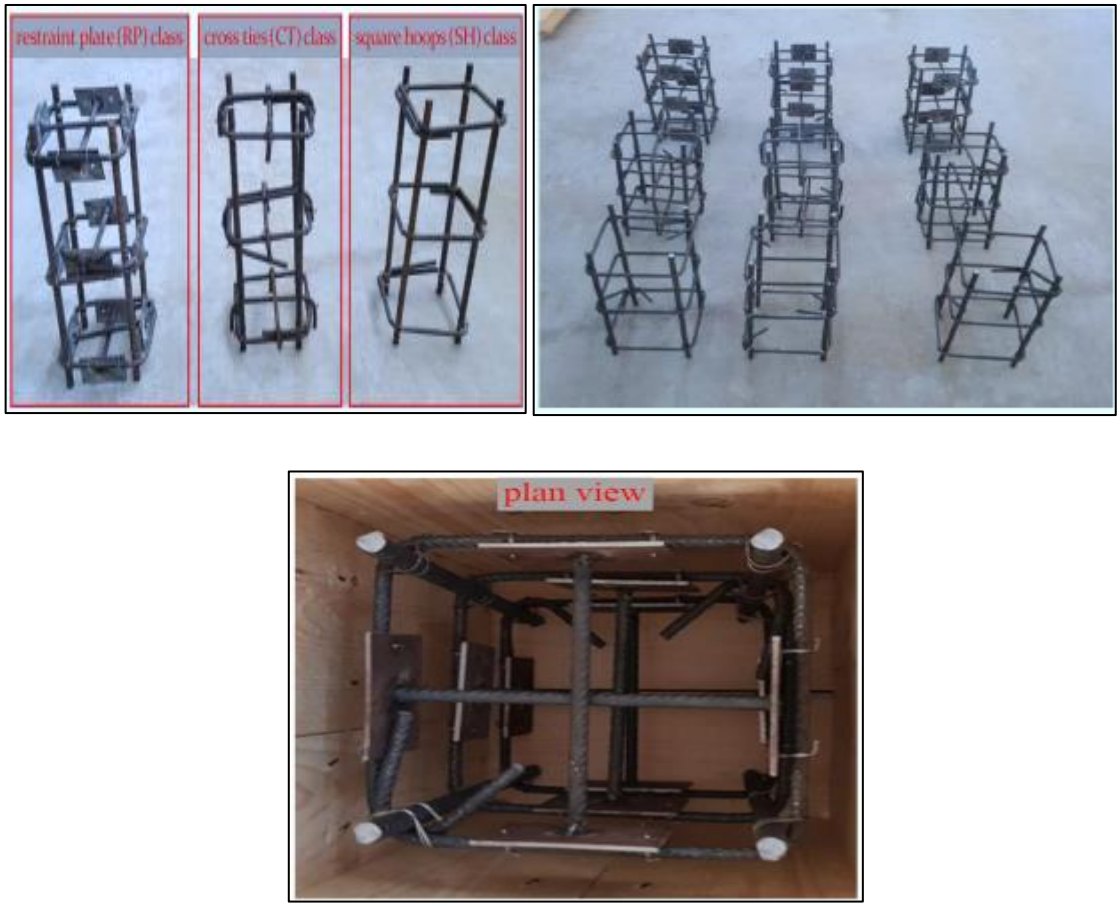

Figure 2. 8 Geometry of the specimens and transverse reinforcement configuration by Dario [23].

Based on experimental results, the configuration of transverse reinforcement with extra cross ties supporting some restraint plates is highly effective in improving the ductility of concrete columns; the mean value of the highest axial strain at collapse has increased in comparison to the ordinary square hoops arrangement.

Mahmoud F. [24] examined the axial load resistance of a reinforced concrete column jacketed by a steel cage. Two un-strengthened specimens and five strengthened ones were tested in a group of seven total specimens using various parameters. The experiment's parameters included the steel jacket's shape (angle, channel, and plates), as well as the quantity and dimensions of batten plates. Additionally, ANSYS version 12 was used for a numerical investigation. For specimens strengthened with angles, the failure load was significantly influenced by the size of the batten plates, but the quantity of batten plates had a greater impact for specimens strengthened with C-channels, according to the researcher.

Syed [25] tested nine specimens of square reinforced concrete columns at one-third scale with a 150mm x 150mm cross sectional dimension and 960mm height. The experiment is carried out for control columns, columns with stirrups and a ferromesh jacket for confinement reinforcement, and columns with a ferromesh jacket acting only as confinement reinforcement. In terms of ductility, stress, strain, axial displacement, load carrying capacity, and other variables, the specimens' overall response was examined. In comparison to a regular control column, the test results show that a column with additional ferromesh wrapped around it as confinement increases its axial strength by 20%. In addition to stirrups, it has been found that columns with ferromesh jackets for confinement reinforcement have better ductility, whereas columns wrapped only with ferromesh as additional confinement fail in a ductile manner.

Ahmed M. [14] carried out an experimental investigation to determine the effectiveness of Expanded Metal Mesh (EMM) section in additional to ordinary tie reinforcement. On the basis of slenderness ratios, 16 square, short column specimens were divided into two groups, and the proposed lateral reinforcement with different tie volumetric ratios was examined. The specimens were cast vertically to represent a construction site, and concentric compression tests were performed on them until they failed. The research revealed that the proposed transverse reinforcement greatly increased the columns' strength and ductility. Additionally, by installing the EMM layer, a significant reduction in ties' volumetric ratio could be accomplished without a reduction in ultimate load.

Kim et al. [26] described how RC columns subjected to cyclic lateral load and constant axial load could be contained by a newly developed spiral-type transverse reinforcement with varying yield strengths. The ductility capacity, energy dissipation, and effective stiffness of the reinforced concrete columns were assessed in comparison to those confined by conventional rectangular reinforcement and developed spiral-type transverse reinforcement. The experimental findings demonstrated that RC column specimens with the newly developed spiral-type lateral reinforcement perform better than specimens with conventional rectangular reinforcement in terms of ductility capacity and energy dissipation, in spite of the reinforcement used for the specimens being reduced by about 27%.

Mariateresa et al. [27] performed an experimental test on a total of 45 full-scale concrete columns that were tested under compression and were reinforced with spirals or hoops and longitudinal steel bars. The columns had a cross-section that was 300 mm wide and 250 mm deep, and there were 18 square columns with a 300 mm side (Figure 2.9). Since each column was about 1300 mm high, its height was at least four times greater than its maximum cross-sectional size. After 28 days, average compressive strengths were measured, and they ranged between 25.2 and 27.8 MPa.

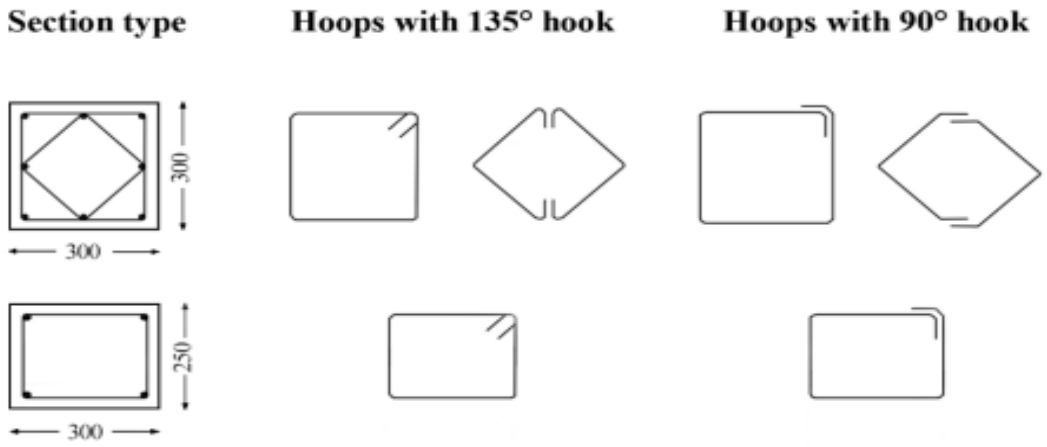

Figure 2. 9 Transverse reinforcement details [27]

12mm and 16mm diameter of steel bar were used for the longitudinal reinforcement, and 8 mm diameter of steel bar were used for the transverse reinforcement. Hoops with a 90° hook and a 135° hook at the end were used to create the specimens (Figure 2.9). In order to prevent direct loading on the longitudinal bars, a concrete layer of roughly 25 mm thickness was cast between the ends of the longitudinal bars and the top and bottom surfaces of the columns. There were three different sets of columns. The first two sets each had transverse reinforcement that was 8 mm in diameter and longitudinal steel bars that were 12 mm in diameter. The first set's spiral and hoop pitch was 150 mm, while the second sets was 75 mm. With 75 mm of space, 8 mm of transverse reinforcement, and longitudinal bars that were 16 mm in diameter, the third set of columns was reinforced. Axial loads were tested on 45 reinforced concrete columns with four volume ratios of transverse reinforcement. We investigated the effects of spiral-reinforced columns and hoops with 135° or 90° hooks on concrete confinement. The test results showed that for a 150 mm hoop pitch, there were only small increases in strength (between 2% and 7%) as a result of the concrete confinement. Smaller improvement was observed for hoops with a 90°

hook, even at a 75 mm pitch. Spirals and hoops with a 135° hook increased strength by about 10–12% at 75 mm pitch. When the pitch was 75 mm and there were rhomboidal hoops or crossties in addition to the perimeter hoops, larger increments (of approximately 11–16%) were obtained. Although the strength increases slightly as the bar diameter goes from 12 mm to 16 mm, failures caused by bar instability decreased, rendering the contribution of longitudinal reinforcement to the confinement of concrete insignificant.

CHAPTER 3 METHODOLOGY

3.1. Finite element method

Through experimental analysis of actual structural members, RC structures' behavior can be evaluated most accurately. Unfortunately, due to cost and time commitment, this is not always possible. A FEM technique has been used as an alternative opportunity in research projects.

ABAQUS, Vector 2, DIANA, ANSYS, and other FEM software have been used to conduct the majority of numerical analyses on structural members in recent years. The proposed modeling approach in this paper was implemented using the commercial finite element analysis software ABAQUS (Simulia, 2022). Its ability to simulate a three-dimensional model and broad range of nonlinear material models led to its selection.

Three main products ABAQUS/CAE, ABAQUS/Standard, and ABAQUS/Explicit come together to form the ABAQUS program suite. To create, analyze, and visualize model output all in one environment using a graphical user interface (GUI), use the first product, which is an entire ABAQUS environment. By importing CAD models created by other compatible products, or by using the software's drawing tools, model geometries can be created in ABAQUS/CAE. In most cases, structures subjected to static, cyclic, and low-speed dynamic effects are simulated using finite elements using ABAQUS/Standard. On the other hand, transient dynamic and highly impactful simulations are performed using ABAQUS/Explicit. For simulations that require preprocessing or postprocessing, ABAQUS/CAE supports both the Standard and Explicit versions [28].

3.2. Geometry

3.2.1. Validation of the FE model of reinforced concrete columns under axial load

Dario [23] experimentally tested reinforced concrete columns under axial load were chosen to be validated in the numerical model. The geometric variables for the finite element analysis were established based on Dario's experiment. Table 3.1 provides an overview of the experiment's specifics and geometric features.

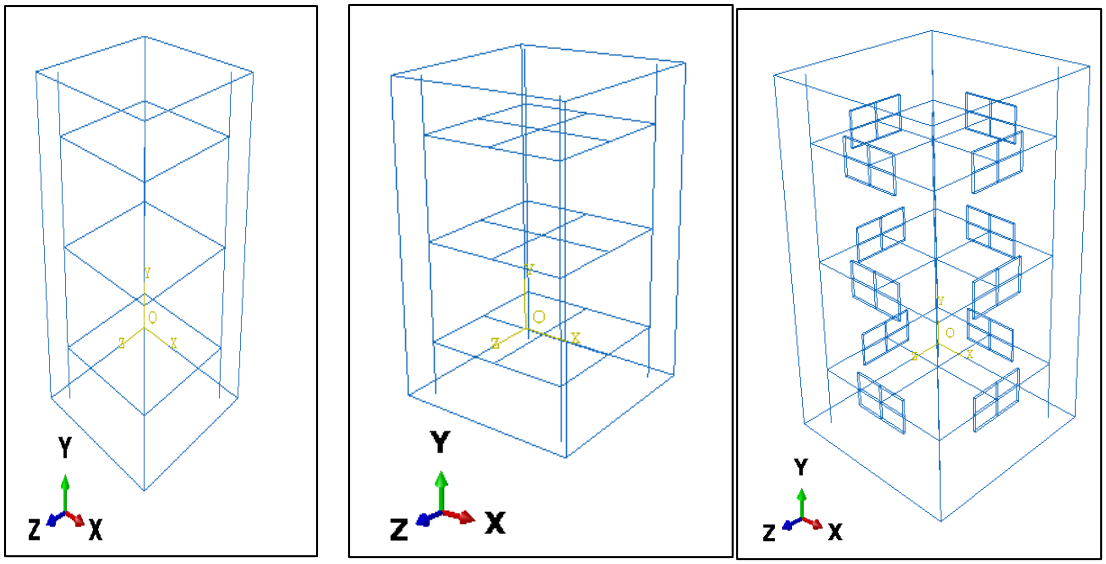

a Square hoop (SH) b. Cross tie (CT) c. Restraint plate (RP)

Figure 3. 1 Geometric characteristics of the chosen specimen by Dario [23]

Table 3. 1 Geometric characteristics of the studied RC column as described by Dario [23].

Model code	SH	SCT	SRP
f'_c (MPa)	25.3	25.3	25.3
Cross section(mm)	250x250	250x250	250x250
f_y main bar (MPa)	450	450	450
f_y stirrups (MPa)	450	450	450
Main bar	4Φ10	4Φ10	4Φ10
Stirrups	Φ8 c/c 130	Φ8 c/c130	Φ8 c/c 130
Restraint Plate lx w x t (mm)			80x40x3

3.2.2. Parametric study of finite element model

In this parametric study, three different layouts of stirrups, namely typical square hoops, stirrups with additional cross ties, and a type of stirrup with additional restraint plates, were used to confine square columns by transverse reinforcement. A finite element program was used to examine the performance of confinement with various geometrical configurations of lateral reinforcement. A column can be classified based on its slenderness ratio. The slenderness ratio determines the buckling strength of a column under compressive loads. If the column is long enough to buckle, it will fail by buckling. If it is too short to buckle, it will fail by crushing. Therefore, the behavior of intermediate columns is somewhere between that of long and short columns. The square specimen is chosen to have a section of 300 x 300 mm and a length of 3000 mm. This parametric investigation's main concern is the confinement effect that various configurations of transverse reinforcement have. Table 3.2 provides a summary of specimen details.

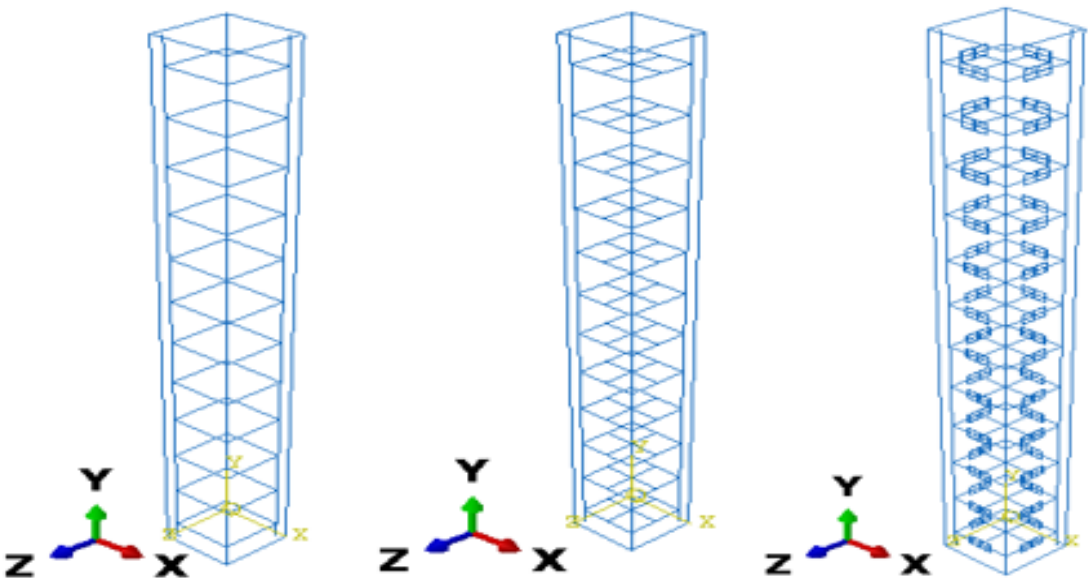

a. Square hoop (SH) b. Cross tie (CT) c. Restraint plate (RP)

Figure 3. 2 Schematic cross-section and reinforcement arrangements created in ABAQUS

3.2.3. Study parameters

The selection of parameters for this parametric study based on the effectiveness of confinement and specific objectives. However, the parameters studied in this research were:

1. Compressive strength of concrete: This parameter affects the overall strength of the column and its ability to resist compressive loads. In medium-strength concrete, two different levels of compressive strength were used to evaluate their impact on the behavior of the column.

2. Spacing of transverse reinforcement: Transverse reinforcement helps to confine the concrete and prevent it from spalling under compressive loads. The spacing between the stirrups varied to determine its effect on the strength and ductility of the column.

3. Longitudinal reinforcement ratio: The amount of longitudinal reinforcement in a column affects its strength, stiffness, and ductility. Different ratios of longitudinal reinforcement were used to evaluate their impact on the column's behavior.

4. Configuration of transverse reinforcement: The configuration of transverse reinforcement can also affect the behavior of the column under compressive loads. Different configurations were considered to determine their effectiveness in improving the strength and ductility of the column.

In order to design a transverse reinforcement scheme that uses additional steel plates for columns with actual dimensions, the following preliminary criteria can be used: the thickness of the plate should be designed based on the lateral expansion of concrete under axial load that corresponds to its ultimate compression capacity, assuming a Poisson's ratio of 0.2; 2) the extension of the plates along the sides should be selected in proportion to the lateral dimensions of the columns and the actual spacing between the stirrups. In the present study, the steel plates have dimensions of 50 x 100 mm and thicknesses of 3 mm,4mm and 5mm while the linking cross-tie is a steel bar with 10 mm diameter.

Overall, in this study, two types of concrete grades with unconfined compressive strengths of 25 MPa and 50 MPa were considered for this parametric study. The spacing between the stirrups was 150 mm and 250mm, and the concrete cover was set to be 25 mm in all specimens. Both the transverse reinforcement and the longitudinal steel rebar had yield

strengths of 420 MPa. 4 ϕ 20mm and 4 ϕ32mm diameter longitudinal bars and transverse reinforcement bars with a diameter of 10mm were used for all cross sections.

Table 3. 2 Detailing of the specimens for parametric study

Model code	SH - 1	SH - 2	SCT - 1	SCT - 2	SRP - 1	SRP - 2
f'_c (MPa)	25	50	25	50	25	50
Cross section (mm)	300x300		300x300		300x300	
f_y main bar (MPa)	420		420		420	
Main bar	4Φ32	4Φ20	4Φ32	4Φ20	4Φ32	4Φ20
f_y stirrups (MPa)	420		420		420	
Stirrups	Φ10		Φ10		Φ10	
Spacing of stirrups (mm)	150	250	150	250	150	250
Linking cross tie			Φ10		Φ10	
Restraint Plate l x w x t (mm)					100x50x3 100x50x4 100x50x5	

3.3. Element type

In the FE, selecting the appropriate element type for each component of the model is crucial because it affects both the accuracy of the results and the length of the analysis. In ABAQUS, a variety of element types are available. Eight-node three-dimensional hexahedral brick elements (C3D8R) with reduced integration were used in this study to simulate concrete (each node has three translational degrees of freedom). Reduced integration elements are chosen to decrease the computation time, which would not be reasonable if high order elements were to occur. Furthermore, reduced integration is suggested in plasticity problems since elements don't exhibit volumetric locking when

plastic flow happens and uncompressible material conduct occur; it was preferred to utilize a finer mesh and low request elements in the analyses. Truss elements T3D2, which have two nodes and are embedded throughout the column body, were used to model the longitudinal and lateral reinforcement. By enclosing the steel bars in a host region (a concrete column), the perfect bond can be precisely defined when using a truss element.

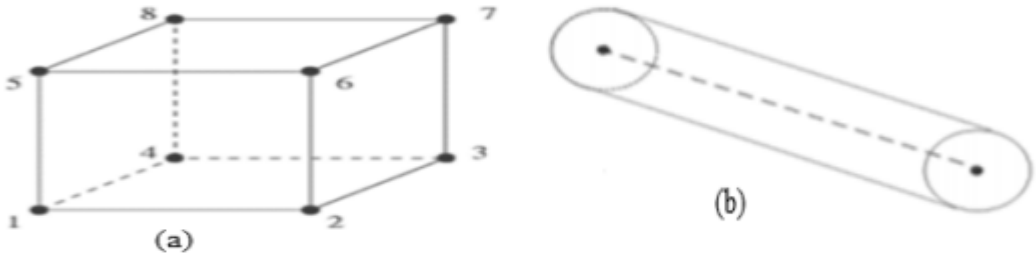

Figure 3. 3 (a) 8-node solid element (C3D8R) for concrete, (b)Truss element(T3D2) elements for reinforcing steel [28]

3.4. Material modeling

The mathematical models that describe the conduct of the materials are referred to as the material models. The material models should show comparable qualities to their physical partners all together for the finite element model to precisely recreate the conduct of the physical framework.

3.4.1. Concrete Damage Plasticity (CDP)

In the most recent decades, a variety of constitutive models have been created, for the prediction of concrete behavior. Three constitutive models, namely the concrete damaged plasticity (CDP) model, the concrete smeared cracking model, and the brittle cracking model, are supported by ABAQUS [29] to simulate the quasi-brittle nature of concrete materials. These three models can accurately simulate a wide range of concrete structures, including beams, trusses, shells, and solids. Depending on the analysis being done, each constitutive model has advantages that can be used.

One of the fundamental problems in structural mechanics recently became the modeling of failure and fracture. The CDP model offers a general capability for modeling and accurately capturing quasi-brittle materials in all types of structures and under various loading conditions. Additionally, concrete structures under monotonic, cyclic, and

dynamic loading can be effectively analyzed using the CDP model [30]. In this study, the concrete is modeled using the concrete damage plasticity model available in ABAQUS (2022). The CDP model may be able to capture all of the concrete's inelastic behavior in tension and compression, including damage characteristics and has a higher convergence capability than the smeared crack approach.

The meaning of the following parameters is necessary for the CDP model in ABAQUS: uniaxial compression response, uniaxial tension response, and ratio of initial biaxial compressive yield stress to initial uniaxial compressive yield stress ($\frac{\sigma_{bo}}{\sigma_{co}}$), ratio of tension meridian and compression meridian deviator second stress invariants (Kc), eccentricity (e) and the dilation angle for the flow potential (ψ).

a. Uniaxial Compressive response

The stress-strain curve of the constitutive connection can be seen in figure 3.4 at the point when the material is subjected to a uniaxial compression load. In a tabular format, the user must enter the stresses (σ_c) inelastic strains (ε_c^{in}) corresponds to stress values, and damage properties (dc) with inelastic strains in tabular format. Therefore, total strain values should be converted to the inelastic strains using equation 3.1.

$$\varepsilon_c^{in} = \varepsilon_c - \varepsilon_{oc}^{el} \qquad 3.1$$

Where $\varepsilon_{oc}^{el} = \frac{\sigma_c}{E_o}$, ε_{oc}^{el} = elastic strain corresponding to the undamaged material and

ε_c = total tensile strain. Further, corrective measures should be taken to ensure that the plastic strain values ($\varepsilon^{\sim pl}$) calculated using equation 3.2 are neither negative nor decreasing with increased stresses [28].

$$\varepsilon^{pl} = \varepsilon_c^{in} - \frac{d_c}{1-d_c}\frac{\sigma_{co}}{E_o} \qquad 3.2$$

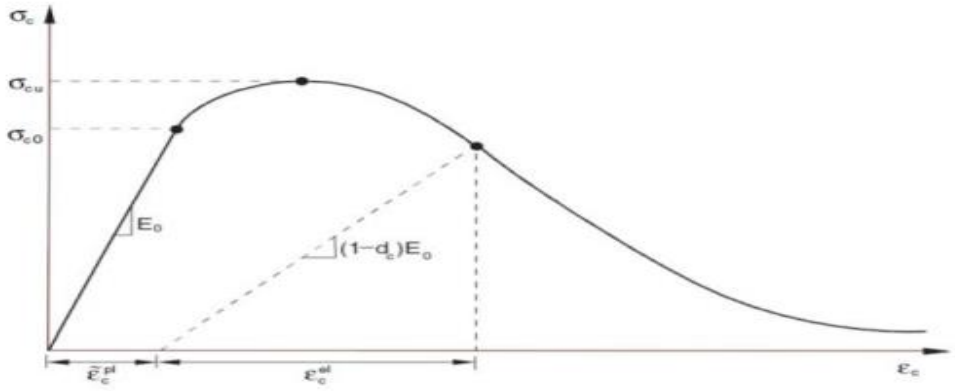

Figure 3. 4 Compressive Stress-Strain Relationship [28].

b. Uniaxial tension response

The curve of the stress-strain on the constitutive relation at the point where the material is subjected to uniaxial tension load is shown in figure 3.5. In order to simulate the full tensile behavior of reinforced concrete, ABAQUS uses a post failure stress-strain relationship for tension-subject concrete. This relationship considers tension stiffening, strain-softening, and reinforcement interaction with concrete. To develop this model, user should input young's modulus (E_o), stress (σ_t), cracking strain (ε_t^{ck}) should be calculated from the total strain using equation 3.3 below:

$$\varepsilon_t^{ck} = \varepsilon^t - \varepsilon_{ot}^{el} \qquad 3.3$$

Where $\varepsilon_{ot}^{el} = \frac{\sigma_t}{E_o}$, ε_{ot}^{el} the elastic strain corresponding to the undamaged material,

ε^t = total tensile strain. [28] checks the accuracy of damage curve using the plastic strain values ($\varepsilon^{\sim pl}$) should be calculated using equation 3.4. Tensile plastic strain values that are negative or decreasing are an indication of incorrect damage curves and may generate error messages prior to analysis [28].

$$\varepsilon_t^{\sim pl} = \varepsilon_t^{ck} - \frac{d_t}{(1- d_t)} \frac{\sigma_{to}}{E_o} \qquad 3.4$$

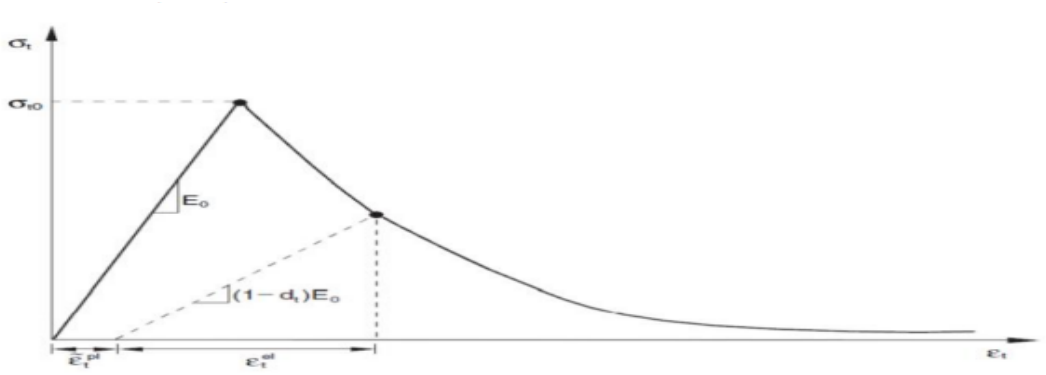

Figure 3. 5 Uniaxial tensile stress strain curve [28].

c. Dilation angle (ψ)

The volumetric strain relative to the shear strain change is measured by the dilation angle. It can also be described as the concrete's internal friction angle or the failure surface's angle of inclination, which evaluates the plastic potential's inclination under intense confining pressure [30]. A range between 30° to 42° of the dilation angle parameters is prescribed for concrete material as indicated by arrangement of crucial examinations performed by various creators [31], [32], [33] and [34]. For the development of this model, a dilation angle of 30° was chosen.

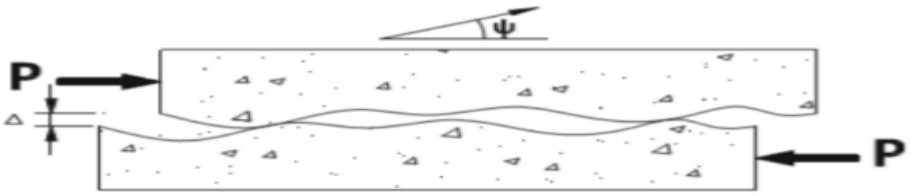

Figure 3. 6 Dilation Angle [35]

d. The flow potential eccentricity (∈)

For the development of this model, the default value of 0.1 was chosen.

e. The ratio of the strength in the biaxial state to the strength in the uniaxial ($\frac{\sigma_{bo}}{\sigma_{co}}$)

The value chosen for the proposed model is 1.16

f. The ratio of the second stress invariant in tension to that in compression (Kc)

The default value of 0.667 given in ABAQUS was selected for the proposed model.

g. The viscosity parameter (μ)

To reduce simulation time and enhance model convergence, it was suggested that a low value for the viscosity parameter be used [30]. The viscosity parameter in ABAQUS is set to zero by default. The value for the proposed model was set at 0.0075 to shorten the simulation time.

Table 3. 3 The values of the Parameters input of the CDP model in the current study

Dilation angle	Eccentricity	$\frac{f_{bo}}{f_{co}}$	k_c	Viscosity parameter
30	0.1	1.16	0.667	0.0075

3.4.2. Steel reinforcement

Both transverse and longitudinal reinforcement in this study involved the use of reinforced steel bars with a yield strength of 420MPa. Standard elastic steel material inputs for the rebar were specified, and these assumptions included the following values for the rebar's elastic modulus (Es) and Poisson ratio (ν): 210 GPa and 0.3, respectively. Up until it gave way, it was believed that the tension reinforcement was elastic. Following yielding, bi-linear behavior with a 1% strain hardening was assumed. Figure 3.7 depicts the usual stress-strain relationship of the reinforcement applied to the numerical model. The following equations are used to express stress and strain:

$f_y = \varepsilon_y E_s$

$f_u = f_y + 0.01Es\ (\varepsilon_u - \varepsilon_y)$ 3.5

Where, f_u is the steel stress corresponding to the ultimate steel strain (ε_u) and

f_y is the steel stress corresponding to the steel yield strain ε_y.

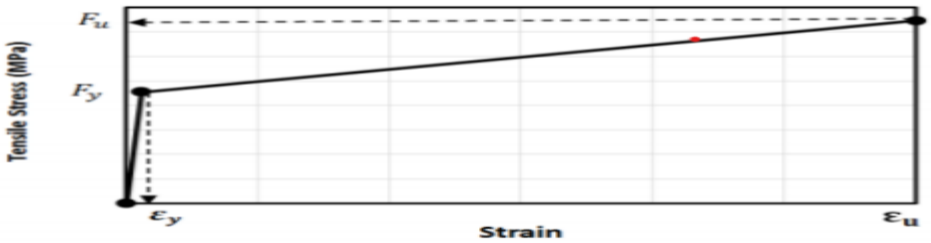

Figure 3. 7 Typical uniaxial stress-strain behavior of reinforcements for the numerical mode [30].

3.5. Interactions and Kinematic Constraints Between Components

The simulated parts need to be connected to one another after being put together. The most important part of a FE analysis is the modeling of contact, which simulates the proper interaction between the components. The kinematic relationship between the various parts must be characterized inside the finite element model in order to guarantee strain compatibility between the various components. In a sense, interaction needed to be specified with the ultimate goal that the equivalent and opposite loading applied between the bodies resulted in one or more bodies deforming jointly This study uses the embedded method, which ensures a perfect bond and displacement continuity between the steel and concrete reinforcement bars [28], [30], [36].

3.6. Boundary condition and Loading

Boundary condition and loading are defined based on the steps in ABAQUS finite element software. In the ABAQUS simulation software, steps are divided into two categories: initial steps and prescribed conditions. The initial step represents the software's default condition.

3.6.1. End boundary conditions

When conducting structural analyses, boundary conditions are used in model regions where rotations and/or displacements are known. During the simulation, such regions may be required to remain fixed (have zero displacement and/or rotation), or they may be allowed to have predetermined, nonzero displacements and/or rotations. The bottom

surface of every specimen in every node of this model was given an ENCASTRE (Fixed) type of boundary.

3.6.2. Loading mechanism

The method of loading structural members using finite elements can be displacement controlled or force controlled. The displacement-controlled method was selected for this study because it can track the behaviors of the RC column after it reaches its maximum loading capacity, providing information on the different types of failure and their underlying mechanisms.

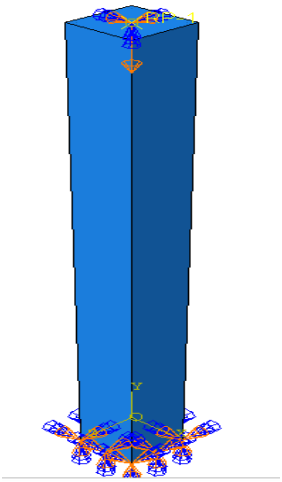

Figure 3. 8 Loading on the reference

3.7. Mesh

The Finite Element Method (FEM) is a numerical technique used for the analysis of structural components. It involves breaking down a complex structure into smaller, simpler parts called finite elements, which are interconnected at discrete points called nodes. Mesh creation is significant for any finite element analysis. It is basic for engineering simulation. This procedure separates the model into various small elements, which is very important to generate accurate results. In finite element modeling, the size of the individual elements has a direct impact on how accurate the outcomes are. Although it takes less time to calculate with larger elements, the results are unrelated to those of experiments. A smaller mesh size will result in more elements, which will increase accuracy. As a result, the analysis will take longer to complete. In order to achieve the desired results, an appropriate mesh size must be chosen. The appropriate mesh size was selected to be 30mm size

elements for the development of this model. The RC column after meshing is depicted in the figure below.

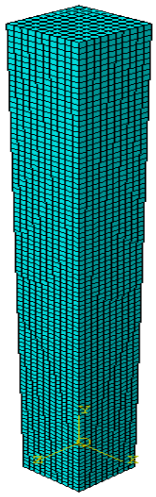

Figure 3. 9 Mesh size of numerical modeling

3.8. Analysis approach

The Newton-Raphson method is used by ABAQUS/Standard to find solutions to nonlinear issues. All of the model's degrees of freedom converge toward the end of each load increment inside of the resistance limits according to Newton-Raphson equilibrium iterations. The residual load vector, which symbolizes the distinction between internal forces (the loads corresponding to the element stresses) and externally applied loads, is once more examined using the Newton-Raphson method. The program performs a linear solution using residual loads while considering the initial stiffness of the structure to confirm the convergence criteria. If the residual load vector is lower than the tolerance value currently in effect, which is 0.5% of the average force over time for the structure, the external and internal forces are in equilibrium. After updating the stiffness matrix and recalculating the residual load vector, a new solution is found if the convergence requirements are not met. Before a solution is taken into consideration to be converged for that load increment, Furthermore, ABAQUS/Standard confirms that the displacement correction is negligibly small in comparison to the overall incremental displacement. It is also regularized to ensure that the convergence checks for the loads and displacements are satisfied [30].

CHAPTER 4 RESULTS AND DISCUSSIONS

4.1. Verification

Numerical validation seeks to simulate the actual behavior of tested specimens and predict the behavior of additional specimens that cannot be experimentally tested. In order to validate the accuracy and reliability of the numerical model, a numerical analysis of concrete columns reinforced with three different layouts of stirrup configurations, namely a closed square hoop (SH), a closed stirrup with additional cross ties (SCT), and a stirrup with additional restraint plates (SRP), under axial compressive loading was performed using ABAQUS and numerical results are compared with three of stirrup layouts, which was experimentally reported by Dario [23]. In terms of mean stress-strain response. The comparison between the experimental and ABAQUS results is shown below.

Figure 4. 1 Experimental setup for Compression test on sample of reinforced concrete column [23]

The FE modeling accurately incorporates all conditions (boundary conditions, loading, material properties, and others) considered in the experimental study. Figure 4.2 and table 4.1 illustrate the ultimate axial stress comparison between the FE simulation and experimental findings using three different stirrup layouts in the model. The FE simulation's output and the experimental output were in good agreement.

A. Mean stress-strain Response

Comparison between Mean stress-strain curves predicted by numerical and experimental results of specimens SH-1, SCT-1 and SRP-1 are presented in figure 4.2(a), figure 4.2(b) and figure 4.2(c) respectively. Similar behaviors between the Mean stress-strain from experiment and ABAQUS simulation indicate good agreement between the FEM analysis results and the actual values provided by Dario [23].

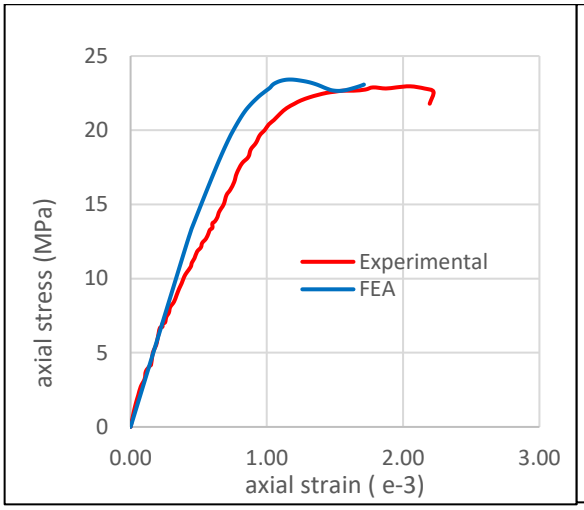

(a)Square hoop (SH)

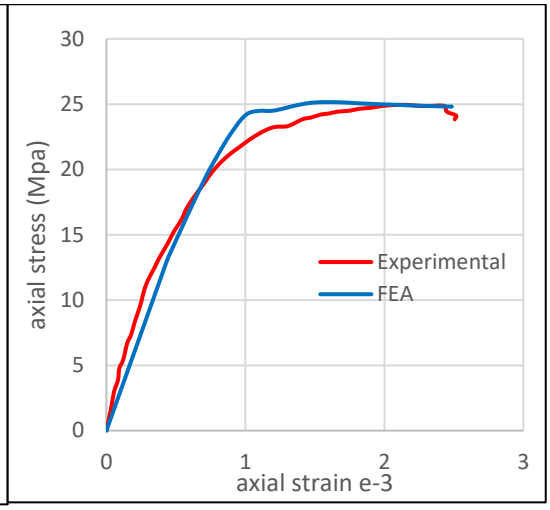

(b) Cross tie (CT)

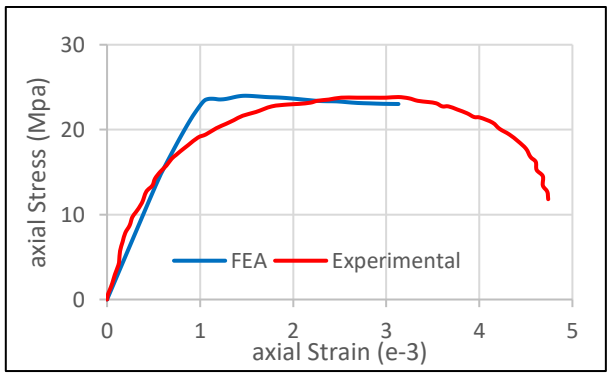

(c) Restraint plate (RP)

Figure 4. 2 Mean stress-strain curve by finite element analysis vs. experimental method

The percentile error E is computed as E $=\left(\frac{N-E}{E}\right)$*100(%), Where E and N represent experimental and numerical results respectively. Table 4.1 presents comparative verification study for peak axial stress result of experimental work together with peak axial

stress from numerical model. The result where clear enough to reflect the acceptable agreement between the experimental and numerical data.

Table 4. 1 Ultimate axial stress comparison between FE and experimental results with three different layouts of stirrups

Model	Peak axial stress (MPa)		Percentage of variation	
	Numerical (FEA)	Experimental	Error (%)	Accuracy (%)
Square hoops (SH-1)	23.5145	22.9584	2.42	97.58
Cross ties (CT – 1)	25.1582	24.938	0.88	99.12
Restraint plate (RP-1)	25.0588	23.838	5.12	94.88

The used software has been verified against an earlier experimental investigation before analyzing the structural behavior of the proposed column specimen. The ultimate axial stress of the modeled reinforced concrete column was found to be 23.51 MPa for typical closed square hoops,25.1582 MPa for a stirrup with additional cross ties, and 25.0588MPa for a stirrup with additional restraint plates, which was closest to the experimental results. The variation between the finite element analysis result and the experimental result was about 2.42% for a square hoop,0.88% for a stirrup with additional cross ties, and 5.12% for a stirrup with additional restraint plates. which was less than 10%, as shown in Figure 4.2. This proved that the ABAQUS program was an appropriate method to predict the performance of axially loaded concrete columns. Moreover, the mean stress-strain curve of the finite element analysis results matched the experimental mean stress-strain curve.

4.2. Parametric Study

In order to better understand the impact of transverse reinforcement arrangement of reinforced concrete column, a thorough parametric study of reinforced concrete column was carried out in this research using finite element package ABAQUS. The parameters compressive strength of concrete, spacing of transverse reinforcement, longitudinal reinforcement ratio, configuration of transverse reinforcement and thickness of a plate analyzed under this study.

Table 4. 2 Properties of the investigated columns

Groups	Column Label	Longitudinal reinforcement Diam.(mm)	Plate dim. (mm)	f_c' (MPa)	f_y, ties (MPa)	Spacing (S) mm
A	C25-SHA150	32	100x50x3	25	420	150
	C25-SCTA150	32		25	420	150
	C25-SRPA150	32		25	420	150
B	C25-SHB250	32	100x50x3	25	420	250
	C25-SCTB250	32		25	420	250
	C25-SRPB250	32		25	420	250
C	C25-SHC150	20	100x50x3	25	420	150
	C25-SCTC150	20		25	420	150
	C25-SRPC150	20		25	420	150
D	C25-SHD250	20	100x50x3	25	420	250
	C25-SCTD250	20		25	420	250
	C25-SRPD250	20		25	420	250
E	C50-SHE150	32	100x50x3	50	420	150
	C50-SCTE150	32		50	420	150
	C50-SRPE150	32		50	420	150
F	C50-SHF250	32	100x50x3	50	420	250
	C50-SCTF250	32		50	420	250
	C50-SRPF250	32		50	420	250
G	C50-SHG150	20	100x50x3	50	420	150
	C50-SCTG150	20		50	420	150
	C50-SRPG150	20		50	420	150
H	C50-SHH250	20	100x50x3	50	420	250
	C50-SCTH250	20		50	420	250
	C50-SRPH250	20		50	420	250
I	C25-SHA150	32	100x50x4	25	420	150
	C25-SCTA150	32		25	420	150
	C25-SRPI150	32		25	420	150
J	C25-SHB250	32	100x50x4	25	420	250
	C25-SCTB250	32		25	420	250
	C25-SRPG250	32		25	420	250
K	C25-SHC150	20	100x50x4	25	420	150
	C25-SCTC150	20		25	420	150
	C25-SRPK150	20		25	420	150
L	C25-SHD250	20	100x50x4	25	420	250
	C25-SCTD250	20		25	420	250
	C25-SRPL250	20		25	420	250

M	C50-SHE150	32	100x50x4	50	420	150
	C50-SCTE150	32		50	420	150
	C50-SRPM150	32		50	420	150
N	C50-SHF250	32	100x50x4	50	420	250
	C50-SCTF250	32		50	420	250
	C50-SRPN250	32		50	420	250
0	C50-SHG150	20	100x50x4	50	420	150
	C50-SCTG150	20		50	420	150
	C50-SRPO150	20		50	420	150
P	C50-SHH250	20	100x50x4	50	420	250
	C50-SCTH250	20		50	420	250
	C50-SRPP250	20		50	420	250
Q	C25-SHA150	32	100x50x5	25	420	150
	C25-SCTA150	32		25	420	150
	C25-SRPQ150	32		25	420	150
R	C25-SHB250	32	100x50x5	25	420	250
	C25-SCTB250	32		25	420	250
	C25-SRPR250	32		25	420	250
S	C25-SHC150	20	100x50x5	25	420	150
	C25-SCTC150	20		25	420	150
	C25-SRPS150	20		25	420	150
T	C25-SHD250	20	100x50x5	25	420	250
	C25-SCTD250	20		25	420	250
	C25-SRPT250	20		25	420	250
U	C50-SHE150	32	100x50x5	50	420	150
	C50-SCTE150	32		50	420	150
	C50-SRPU150	32		50	420	150
V	C50-SHF250	32	100x50x5	50	420	250
	C50-SCTF250	32		50	420	250
	C50-SRPV250	32		50	420	250
W	C50-SHG150	20	100x50x5	50	420	150
	C50-SCTG150	20		50	420	150
	C50-SRPW150	20		50	420	150
X	C50-SHH250	20	100x50x5	50	420	250
	C50-SCTH250	20		50	420	250
	C50-SRPX250	20		50	420	250

4.2.1 Effect of configuration of transverse reinforcement

A parametric study was carried out to investigate the confining effect of different configurations of transverse reinforcement on an axially loaded concrete column. Figure 4.3 displays the strength of three different stirrup layouts for reinforced concrete columns. namely SH, SCT, and SRP on stress - strain curves. Keeping the following parameters (i.e., compressive strength of concrete, longitudinal reinforcement ratio, spacing of transverse reinforcement, and thickness of a plate) constant, the effects of an arrangement of lateral reinforcement on ultimate load resistance for each group of specimens have been investigated.

Table 4.3 provides a summary of the peak compressive stress for different geometrical configurations of transverse reinforcement in reinforced concrete columns. Based on the data in the table 4.3 the results were discussed with respect to strength and confinement effect of reinforced concrete columns.

Reinforcement, such as stirrups, helps to increase the compressive strength of the reinforced concrete column. The stirrups provide additional support and prevent the concrete from failing under compression. When comparing the peak compressive stresses for each group, we can see that columns reinforced with stirrups SRP exhibit the highest values. This suggests that the stirrups SRP (stirrups with additional restraint plates) are more effective in enhancing the compressive strength of the columns compared to stirrups SH (square hoops) and SCT (a stirrup with additional cross ties).

Confinement refers to the ability of the reinforcement to confine and strengthen the concrete. It helps to prevent the concrete from spalling or failing under lateral pressure. When comparing the peak compressive stresses for each group, the result shows that columns reinforced with stirrups SRP have the highest values. This indicates that the stirrups with additional restraint plates provide better confinement compared to stirrups SH and SCT. The reinforcement helps to confine the concrete and prevent it from expanding or cracking under pressure.

Overall, a stirrup with a restraint plates has an impact on reinforced concrete columns behavior. It has been demonstrated that stirrups with restraint plates very effective in enhancing both the compressive strength and confinement of the columns compared to square hoops and a stirrup with additional cross ties. This means that columns reinforced

with stirrups involving restraint plates were more likely to withstand higher loads and resist failure under compression.

Table 4. 3 Result Summary of Peak compressive Stress – strain of specimens for different geometrical configuration of transverse reinforcement

Group of Specimens		SH	SCT	SRP	Percentage variation with respect to SH	
					SCT (± %)	SRP (± %)
A	f_c' = 25MPa ρ = 3.57% S = 150mm	38.91	42.01	47.79	+7.94	+22.81
B	f_c' = 25MPa ρ = 3.57% S = 250mm	38.89	40.23	40.53	+3.44	+4.21
C	f_c' = 25MPa ρ = 1.39% S = 150mm	35.61	42.27	45.82	+18.70	+28.67
D	f_c' = 25MPa ρ = 1.39 % S = 250mm	35.53	38.56	38.16	+8.55	+7.42
E	f_c' = 50MPa ρ = 3.57% S = 150mm	63.24	67.08	71.09	+6.07	+12.41
F	f_c' = 50MPa ρ = 3.57% S = 250mm	63.18	67.03	67.07	+6.09	+ 6.17
G	f_c' = 50MPa ρ = 1.39% S = 150mm	60.47	65.13	70.04	+7.71	+15.83
H	f_c' = 50MPa ρ = 1.39% S = 250mm	60.39	64.23	64.87	+6.36	+7.43

± % Indicates percentage of increment in value relative to that of a square hoop peak stress

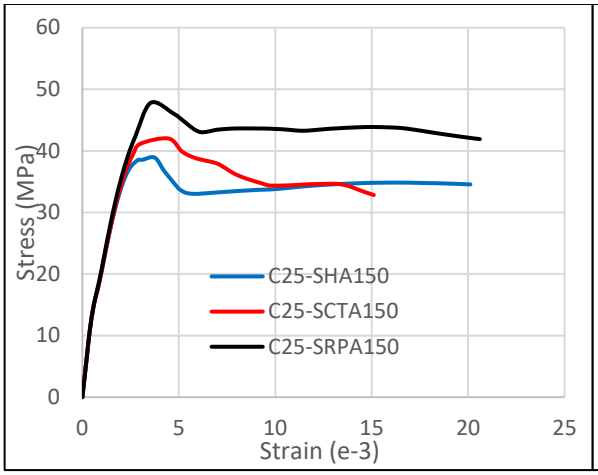

a. Group A

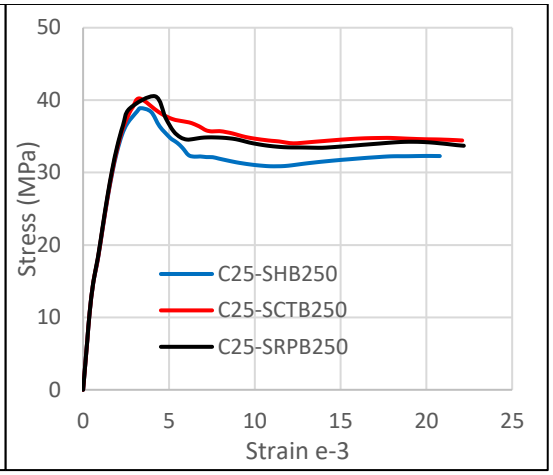

b. Group B

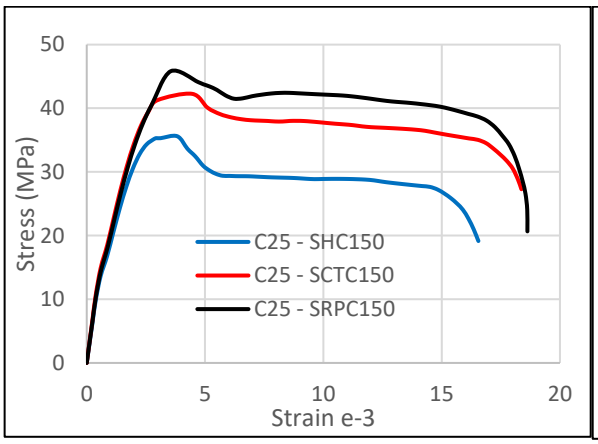

c. Group C

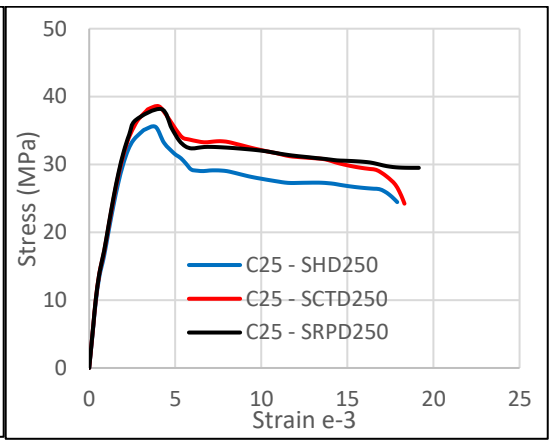

d. Group D

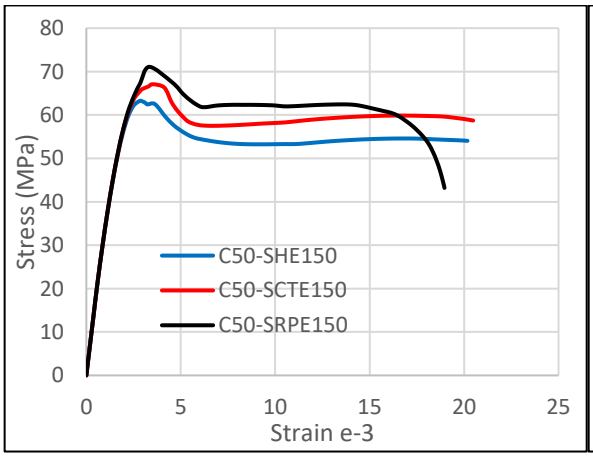

e. Group E

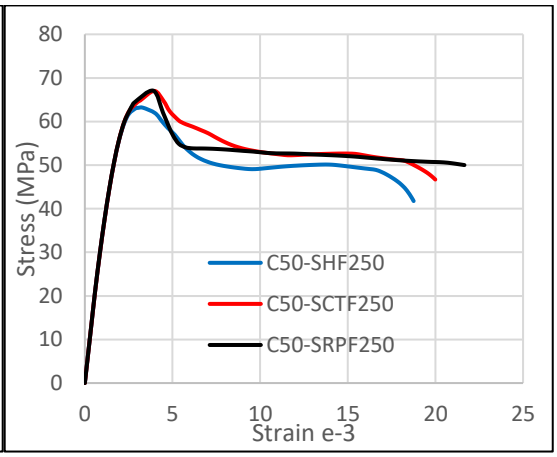

f. Group F

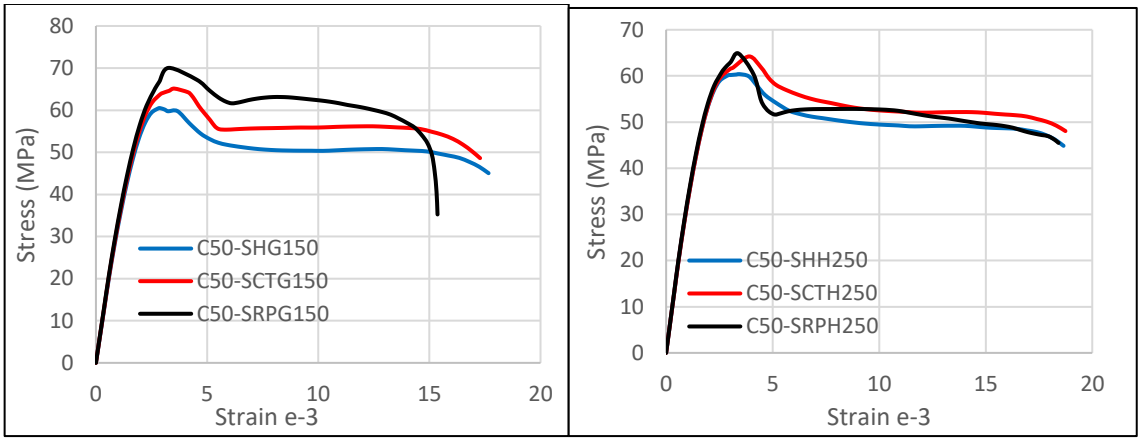

g. Group G h. Group H

Figure 4. 3 Mean Stress – Strain Curve for different geometrical configuration of transverse reinforcement

4.2.2. Effect of Compressive strength of concrete

High strength concrete exhibits less lateral expansion under axial compressive pressures than normal strength concrete because it has higher elasticity modules and less internal cracking. Higher strength concrete is less ductile than lower strength concrete. Additionally, the Poisson effect makes the lateral expansion in lower strength concrete greater for a given amount of axial loading. The hoops will be subjected to more stress than they would in higher strength concrete because the confining pressure initiates earlier in lower strength concrete [37].

As shown in table 4.4, a square column reinforced with three different layouts of stirrups, namely, square hoops (SH), a stirrup with additional cross ties (SCT), and a type of stirrups with additional restraint plates (RP) with the same arrangement of longitudinal reinforcement and the impact of concrete's compressive strength on the ultimate load resistance of reinforced concrete columns has been studied on the performance of the RC column under axial load, while controlling other variables.

In pairs of groups the peak axial load increases when the concrete compressive strength changes from C25 to C50. This indicates that increasing the compressive strength enhances the overall strength of the column. Specifically, as the compressive strength changes from C25 to C50, the effect of stirrups with additional restraint plates (SRP) slightly higher than a square hoops (SH), a stirrup with additional cross ties (SCT). The

increase in peak axial load can be attributed to the improved capacity of the concrete to withstand compressive forces.

The increase in peak axial load with higher compressive strength can be attributed to the improved confinement effect provided by stirrups. As the compressive strength increases, the concrete becomes stronger and more resistant to lateral expansion. This allows the stirrups to effectively confine the core and prevent separation from the cover.

In summary, the result in table 4. 4 indicates that increasing the compressive strength of the concrete from C25 to C50 generally improves the load-carrying capacity of reinforced concrete columns. This increase in compressive strength allows the columns to withstand greater loads before failure. The effectiveness of stirrups in providing confinement remains consistent regardless of the compressive strength or reinforcement details.

Table 4. 4 Result Summary of Peak axial load – Displacement of specimens for C = 25MPa and C=50MPa

			f_c' = 25MPa		f_c' = 50MPa		Percentage of variation
Groups of specimens	Designation		Peak Axial load (kN)	Displacement at peak load (mm)	Peak Axial load (kN)	Displacement at peak load (mm)	Peak Axial load (%)
A with E	SH	ρ = 3.57% S= 150mm	4664.29	8.1425	6960.55	8.1425	+49.23
	SCT		4759.83	8.1425	7036.14	8.1425	+47.82
	SRP		4856.82	8.1425	7088.36	7.8425	+45.94
C with G	SH	ρ = 1.39% S= 150mm	3837.84	8.1425	6133.24	8.1425	+59.81
	SCT		3933.43	8.1425	6208.83	8.1425	+57.85
	SRP		4046.86	8.1425	6289.3	7.8425	+55.41
B with F	SH	ρ = 3.57% S= 250mm	4575.38	8.1425	6886.02	8.1425	+50.50
	SCT		4641.24	7.8425	6919.8	8.1425	+49.09
	SRP		4595.06	7.3425	6876.51	7.8425	+49.65
D with H	SH	ρ = 1.39 % S= 250mm	3753.85	8.1425	6060.84	8.1425	+61.46
	SCT		3817.4	7.8425	6094.72	8.1425	+59.66
	SRP		3771.22	7.3425	6051.15	7.8425	+60.46

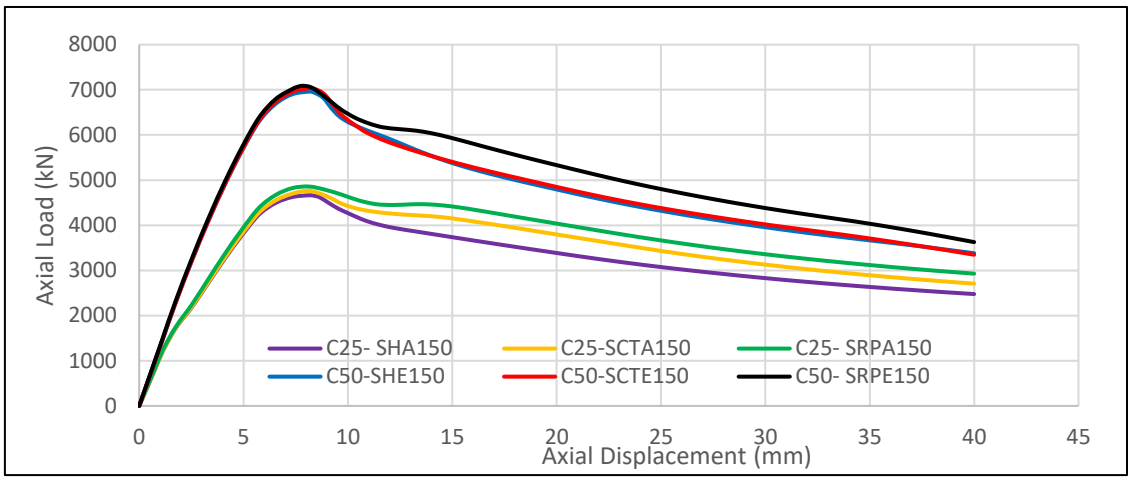

a. Group A with Group E

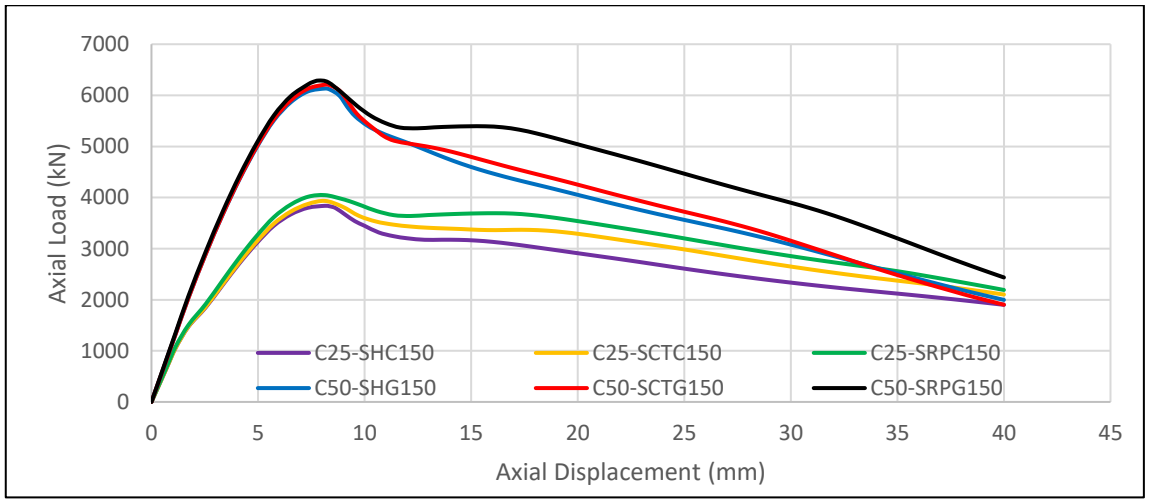

b. Group C with Group G

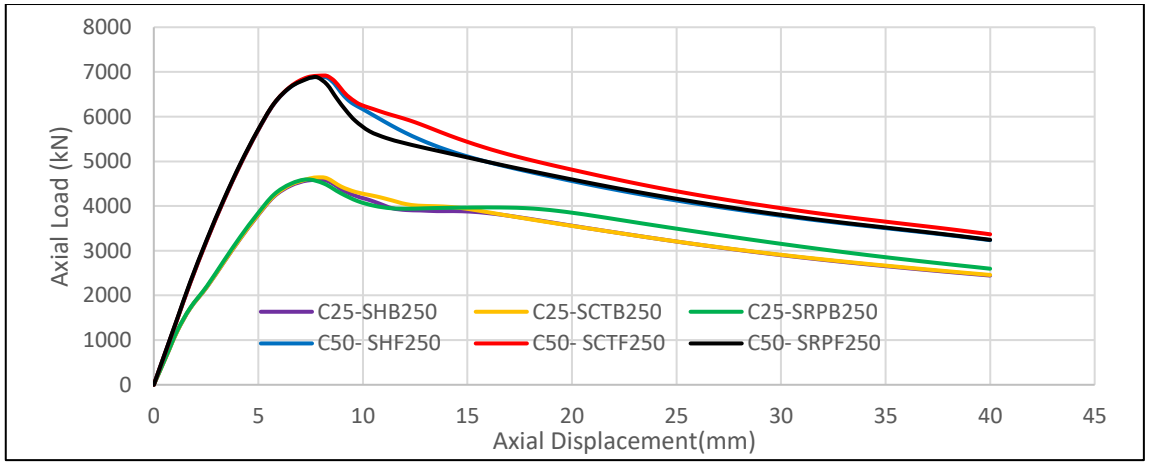

c. Group B with Group F

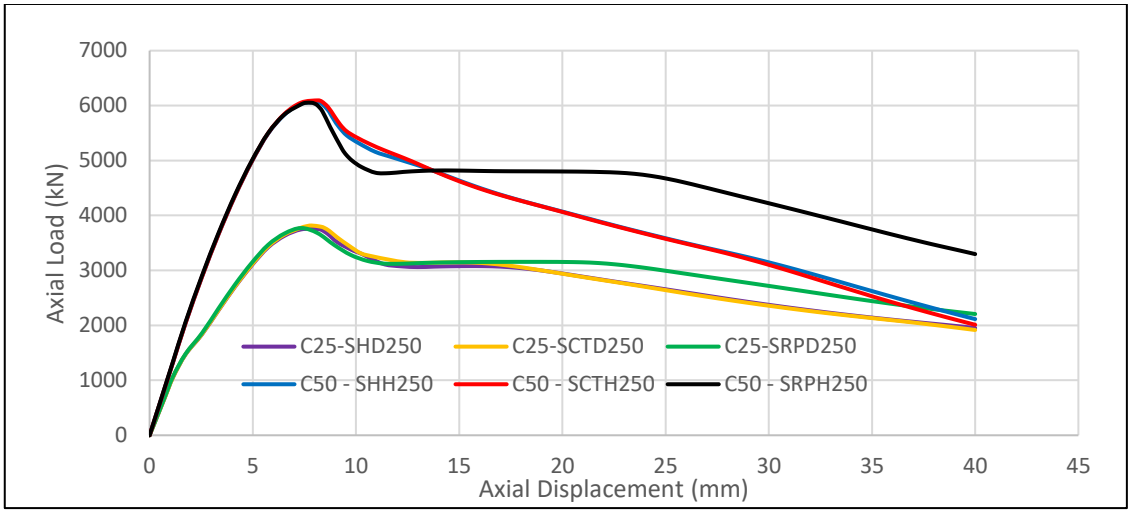

d. Group D with Group H

Figure 4. 4 Axial Load -Displacement curve of specimens for different compressive strength of concrete

4.2.3. Effect of longitudinal reinforcement ratio

In the present study, the influence of longitudinal reinforcing ratio was investigated by developing FE models for all specimens. Each specimen was modeled at different values of longitudinal reinforcing ratio of 1.39% and 3.57% at different values of compressive strength of concrete 25MPa and 50MPa.

When the longitudinal reinforcement ratio increases from 1.39% to 3.5%, there is an increase in the peak axial loads for all three different layouts of stirrups, namely square hoops (SH), a stirrup with additional cross ties (SCT), and a stirrup with additional restraint plates (SRP). Based on table 4.5, the ultimate load capacity of a reinforced concrete column increased by an average around 21% for C25 and 13 % for C50 as the longitudinal reinforcement ratio increased from 1.39% to 3.5%.

In summary, the result in table 4. 5 indicates that increasing the longitudinal reinforcing ratio from 1.39% and 3.57%, generally improves the load-carrying capacity of reinforced concrete columns. This indicates that increasing the longitudinal reinforcement ratio enhances the column's strength and its ability to withstand axial loads.

Table 4. 5 Result Summary of Peak axial load – Displacement of specimens for $\boldsymbol{\rho}$ = 3.57% and $\boldsymbol{\rho}$ = 1.39%

			ρ = 3.57%		ρ = 1.39%		Percentage of variation
Groups of specimens	Designation		Peak Axial load (kN)	Displacement at peak load (mm)	Peak Axial load (kN)	Displacement at peak load (mm)	Peak Axial load (%)
A with C	SH	f_c' = 25MPa S = 150mm	4664.29	8.1425	3837.84	8.1425	+21.53
	SCT		4759.83	8.1425	3933.43	8.1425	+21.01
	SRP		4856.82	8.1425	4046.86	8.1425	+20.01
E with G	SH	f_c' = 50MPa S = 150mm	6960.55	8.1425	6133.24	8.1425	+13.49
	SCT		7036.14	8.1425	6208.83	8.1425	+13.32
	SRP		7088.36	7.8425	6289.3	7.8425	+12.71
B with D	SH	f_c' = 25MPa S= 250mm	4575.38	8.1425	3753.85	8.1425	+21.89
	SCT		4641.24	7.8425	3817.4	7.8425	+21.58
	SRP		4595.06	7.3425	3771.22	7.3425	+21.85
F with H	SH	f_c' = 50MPa S = 250mm	6886.02	8.1425	6060.84	8.1425	+13.61
	SCT		6919.8	8.1425	6094.72	8.1425	+13.54
	SRP		6876.51	7.8425	6051.15	7.8425	+13.64

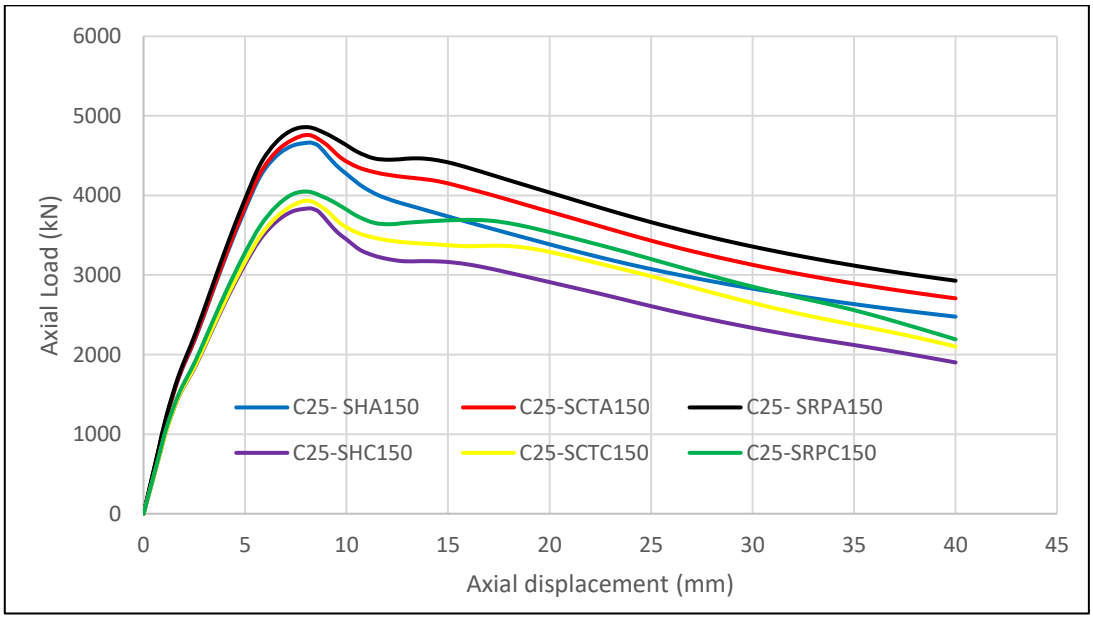

a. Group A with Group C

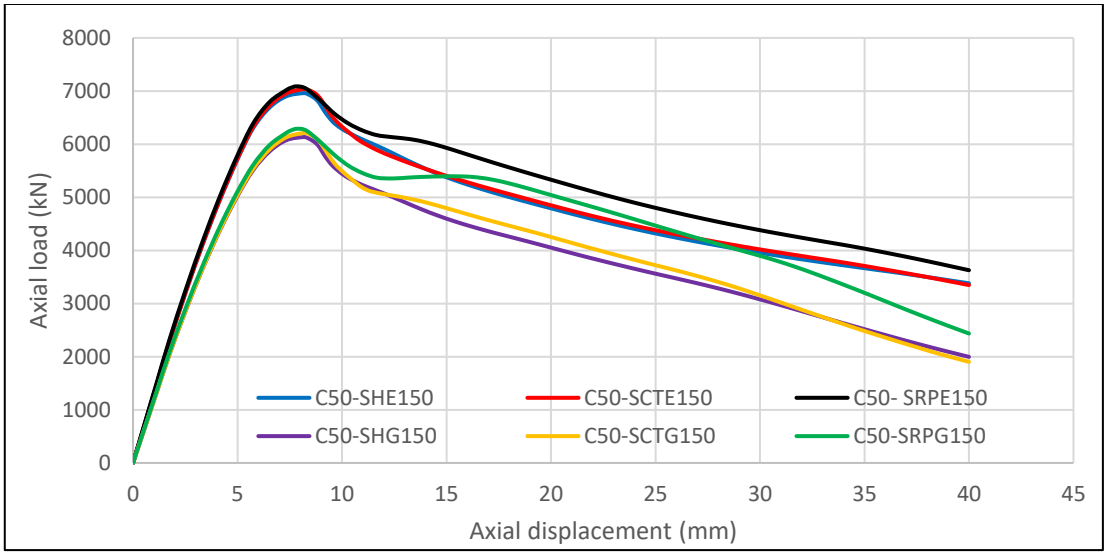

b. Group E with Group G

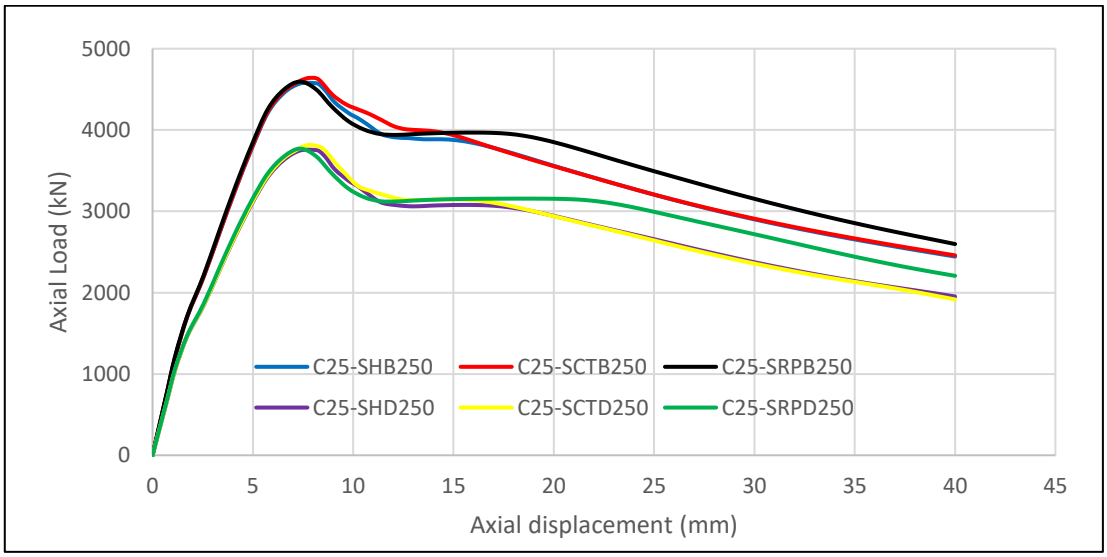

c. Group B with Group D

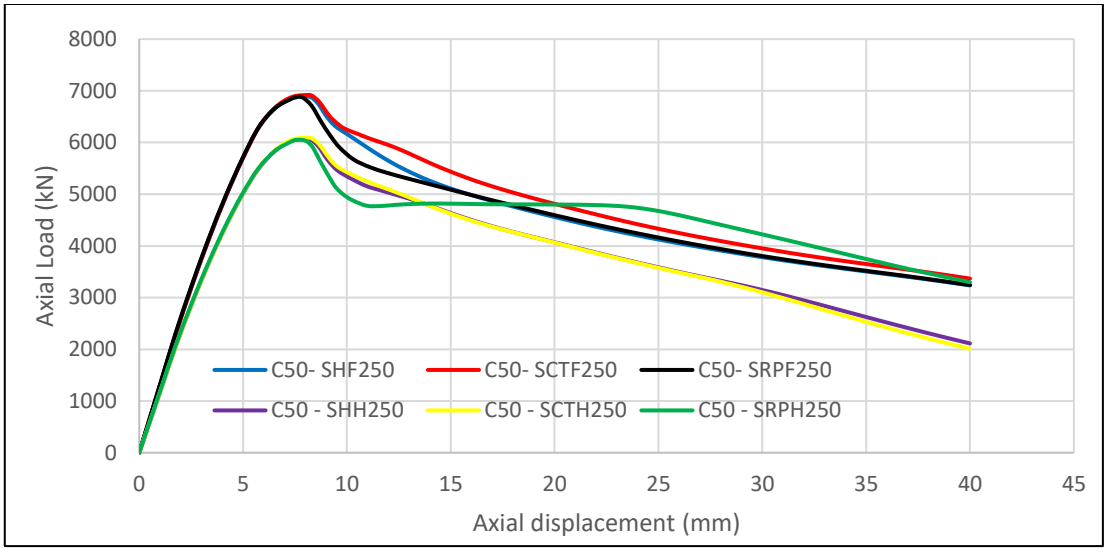

d. Group F with Group H

Figure 4. 5 Axial Load -Displacement curve of specimens for different longitudinal reinforcement ratio

4.2.4. Spacing of Transverse Reinforcement

It has been conclusively established through numerous earlier studies that the transverse reinforcement spacing in reinforced concrete columns significantly affects the concrete's confined compressive strength. To compute and see the effect of spacing of transverse reinforcement in reinforced concrete columns, the specimens were grouped as described in table 4.2.

Based on the results in table 4.6, when the spacing of the transverse reinforcement changes from 150mm to 250mm, there is a decrease in the peak axial loads for all three different layouts of stirrups. This decrease in peak axial load can be attributed to the reduced confinement provided by the transverse reinforcement at a larger spacing. The load carrying capacity of the column confined with additional restraint plates is relatively increased when the spacing between transverse reinforcements is closed to 150mm from 250mm. A stirrup with additional cross ties offers a modest enhancement of ultimate load capacity as compared to the conventional square hoop configuration.

A large spacing of transverse reinforcement in a reinforced concrete column can lead to reduced confinement, decreased load carrying capacity, and increased risk of brittle failure. In terms of column strength, a decrease in peak axial load indicates a decrease in

the ability of the column to withstand axial loads. Furthermore, the larger spacing of transverse reinforcement can reduce confinement of the concrete core. This can result in decreased ductility and resistance to lateral loads, making the column more susceptible to premature failure. Overall, the decrease in peak axial load when the spacing of transverse reinforcement increases from 150mm to 250mm suggests a potential decrease in column strength.

Table 4. 6 Result Summary of Peak axial load – Displacement of specimens at peak load for different transverse reinforcement spacing

			c/c = 150mm		c/c = 250mm		Percentage of variation
Groups of specimens	Designation		Peak Axial load (kN)	Displacement at peak load (mm)	Peak Axial load (kN)	Displacement at peak load (mm)	Peak Axial load (%)
A with B	SH	f_c' = 25MPa ρ = 3.57%	4664.29	8.1425	4575.38	8.1425	1.94
	SCT		4759.83	8.1425	4641.24	7.8425	2.56
	SRP		4856.82	8.1425	4595.06	7.3425	5.70
C with D	SH	f_c' = 25MPa ρ = 1.39%	3837.84	8.1425	3753.85	8.1425	2.24
	SCT		3933.43	8.1425	3817.4	7.8425	3.04
	SRP		4046.86	8.1425	3771.22	7.3425	7.31
E with F	SH	f_c' = 50MPa ρ = 3.57%	6960.55	8.1425	6886.02	8.1425	1.08
	SCT		7036.14	7.8425	6919.8	8.1425	1.68
	SRP		7088.36	7.3425	6876.51	7.8425	3.08
G with H	SH	f_c' = 50MPa ρ = 1.39 %	6133.24	8.1425	6060.84	8.1425	1.19
	SCT		6208.83	8.1425	6094.72	8.1425	1.87
	SRP		6289.3	7.8425	6051.15	7.8425	3.94

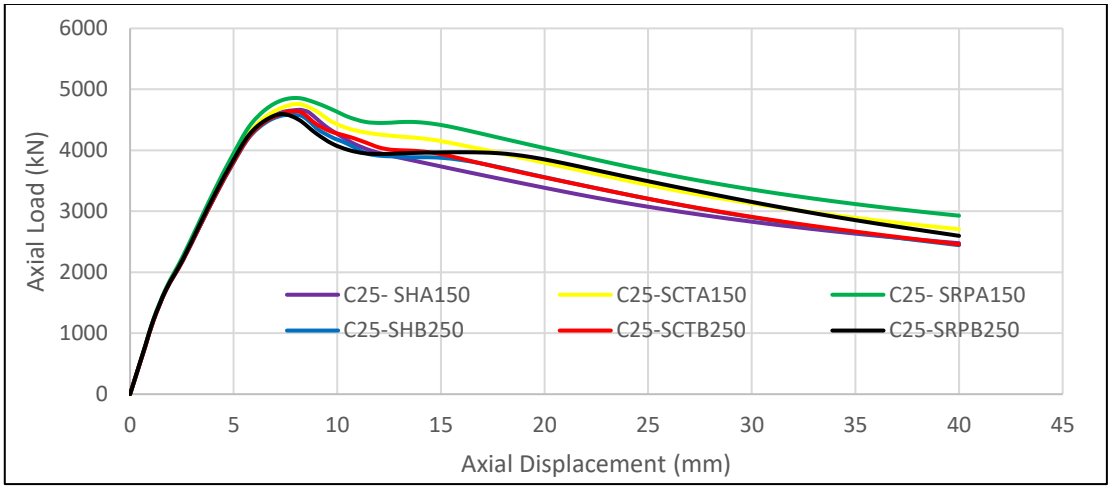

Group A with Group B

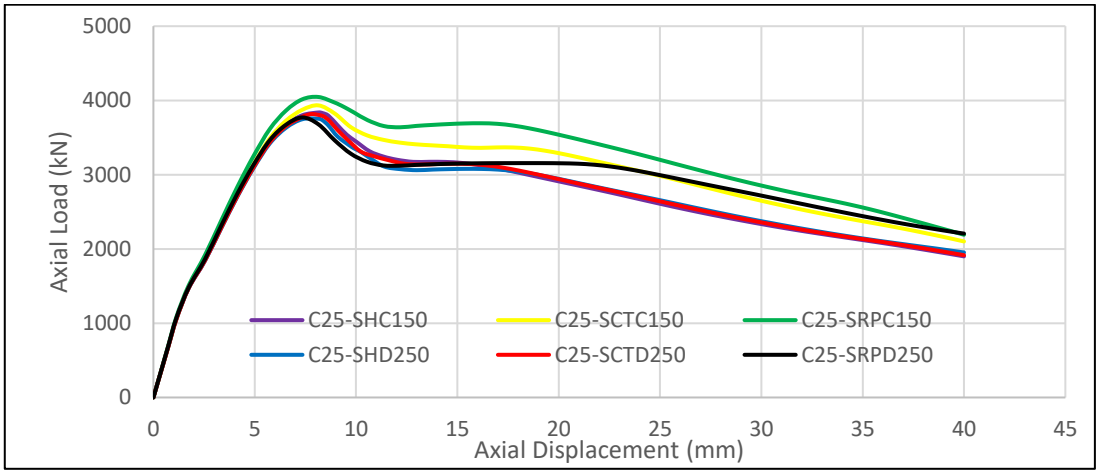

b. Group C and Group D

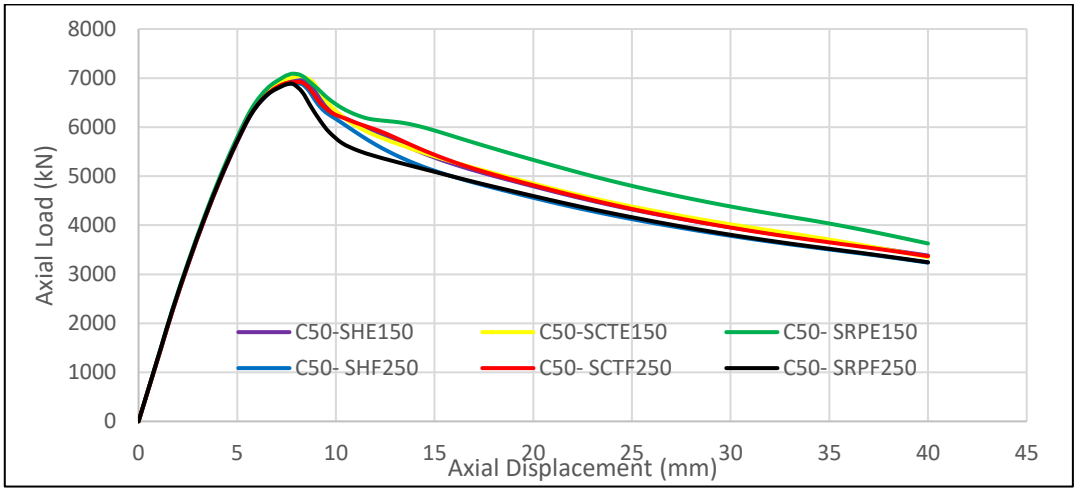

c. Group E and Group F

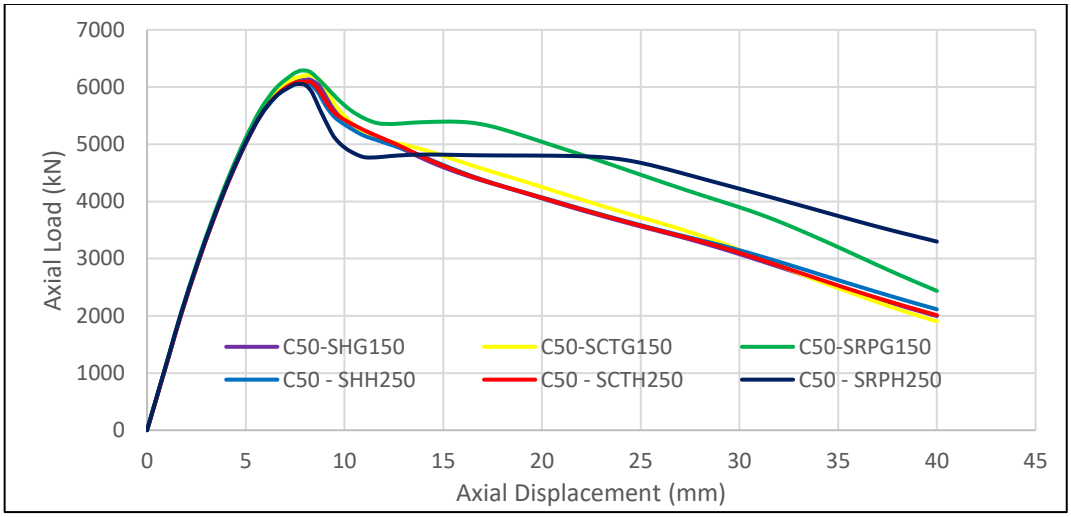

d. Group G and Group H

Figure 4. 6 Axial Load -Displacement curve of specimens for different transverse reinforcement spacing

4.2.5 Effect of plate thickness

Based on the result in table 4.7, It can be observed that as the thickness of the restraint plates (SRP) increases from 3 to 5mm in each group, the peak axial load generally decreases slightly. This suggests that increasing the thickness of the restraint plates may not necessarily result in higher peak loads.

There could be several reasons for this observation. One possible explanation is that as the thickness of the restraint plates increases, it may restrict the lateral expansion of the concrete core, leading to a decrease in the overall load-carrying capacity of the column. Another reason could be that increasing the thickness of the restraint plates may result in a reduction in the effective confinement provided by the stirrups, leading to a decrease in the peak axial load.

Table 4. 7 Result Summary of Peak axial load – Displacement of specimens for different plate thickness

Groups of specimens	Designation		Peak Axial load (kN)	Displacement at peak load (mm)	Percentage of variation (%) With respect to a RP with t=3mm
Group A	C25 – SRPA150	ρ = 3.57%	4856.82	8.1425	
Group I	C25 – SRPI150	S= 150mm	4822.05	8.1425	-0.7
Group Q	C25 – SRPQ150	f_c' = 25MPa	4811.40	8.1425	-0.93
Group D	C25 – SRPD250	ρ = 1.39%	3771.22	7.3425	
Group L	C25 – SRPL250	S= 250mm	3749.44	7.3425	-0.58
Group T	C25 – SRPT250	f_c' = 25MPa	3731.11	7.3425	-1.06
Group E	C50 – SRPE150	ρ = 3.57%	7088.36	7.8425	
Group M	C50 – SRPM150	S= 150mm	7042.03	7.8425	-0.65
Group U	C50 – SRPU150	f_c' = 50MPa	6977.80	7.8425	-1.56

± % Indicates percentage of decrement in value relative to that of a RP with t=3mm

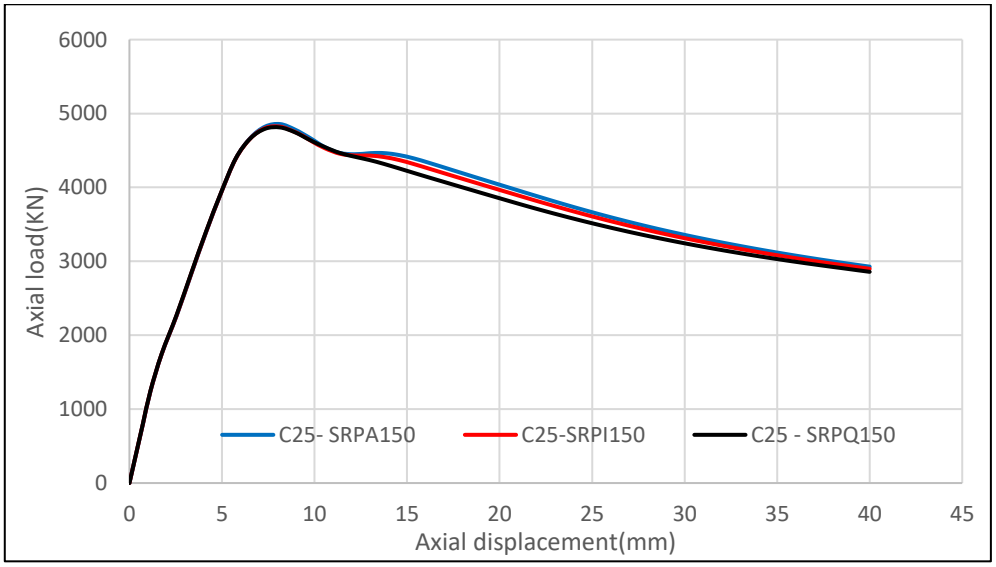

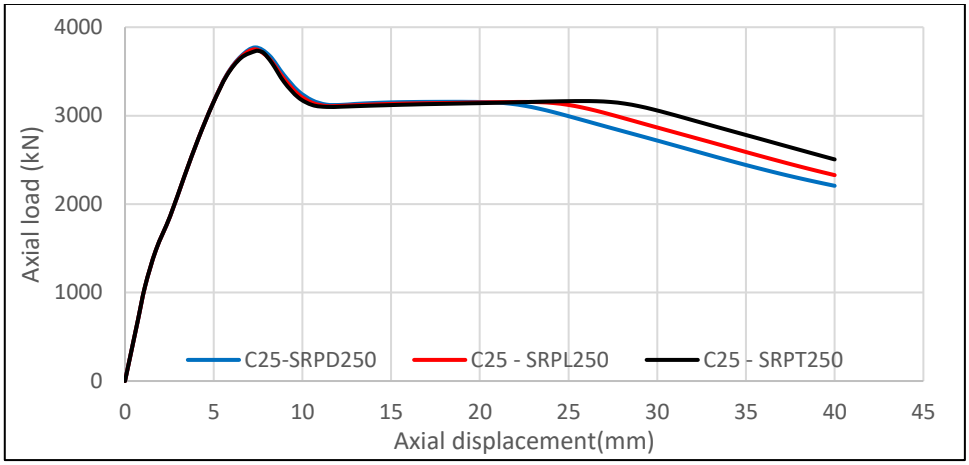

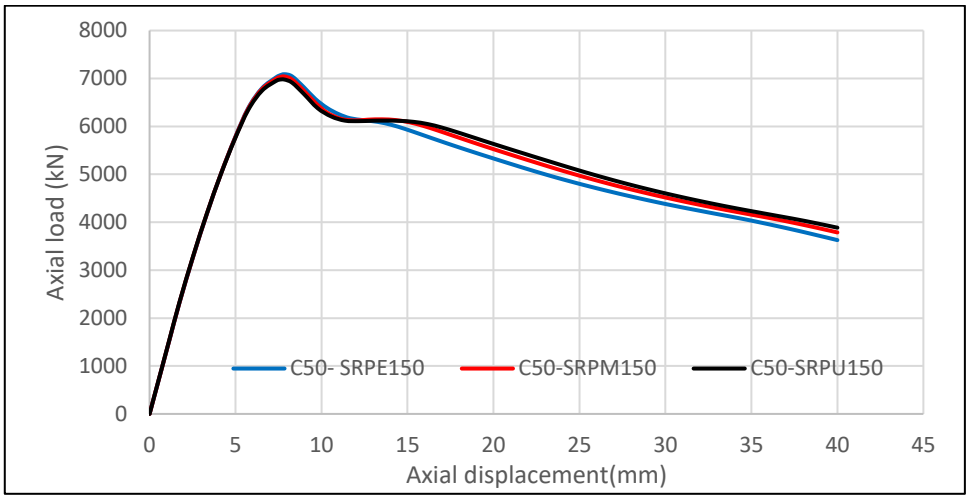

Figure 4. 7 Axial Load -Displacement curve of specimens for different plate thickness

4.2.6 Evaluation of Column Deformability

The deformability of concrete beyond the peak stress is significantly affected by the behavior of longitudinal reinforcement. longitudinal reinforcement in concrete is lateral restrained against buckling. However, the longitudinal reinforcement becomes susceptible to buckling when the cover concrete spalls at roughly the level of the peak stress. The lateral support that transverse reinforcement offers at this load stage starts to matter. The stability of longitudinal reinforcement between the ties is ensured if the amount of lateral reinforcement is sufficiently high in comparison to the length of longitudinal reinforcement that is not supported. To continue providing effective confinement against the lateral expansion of concrete, a stable reinforcement cage is necessary Therefore, the amount of transverse reinforcement, expressed in terms of reinforcement ratio (ρ), play a major role on the descending slope of the stress-strain relationship [38].

Column deformation exhibit the ability of columns to deform without a significant loss of strength. In this study program, its ductility was examined into the deformability of the specimens tested. The ductility of columns was determined in terms of the axial strain ductility ratio which is the ratio between the axial strains of the confined core at a certain level of loading on the descending part to the axial strain of the confined core at the ultimate strength [39]. The strain-to-ductility ratio is determined as follows: [40].

$$u_{85d} = \frac{\epsilon_{85d}}{\epsilon_{cc}}$$

where: u_{85d} = Axial strain ductility ratio corresponding to ϵ_{85d}

ϵ_{85d} = Axial strain corresponding to the 85 % of the ultimate compressive load on the descending part

ϵ_{cc} = Axial strain corresponding to the ultimate compressive load.

The table 4.8 provides a summary of the axial strain ductility ratio for different geometrical configurations of transverse reinforcement in reinforced concrete columns.

From the table 4.8, it can be observed that as the spacing of transverse reinforcement changes from 150mm to 250mm, there is an overall decrease in ductility ratio. For example, the ductility ratio of specimen C25-SRPA150 is 2.73 and the ductility ratio of specimen C25-SRPB250 is 1.34. Similar trends can be observed in all other specimens. In

section of table 4.8 in particular, passing from a square hoops (SH) to a stirrup with additional cross ties (SCT) and a stirrup with additional restraint plates (SRP) configuration there is an increase in the ductility ratio of specimen under 150mm spacing of transverse reinforcement. Since a larger spacing of transverse reinforcement may result in reduced confinement, which can limit the ability of the column to undergo large deformations. This could lead to a decrease in ductility.

Similarly, when the longitudinal reinforcement ratio changes from 1.39% to 3.5%, it can also impact the ductility of the column. For example, the ductility ratio of specimen C25-SRPC150 is 3.13 and the ductility ratio of specimen C25-SRPA150 is 2.73. from this it can be seen that the ductility ratio decreases as longitudinal reinforcement ratio changes from 1.39% to 3.5%. hence Increasing the longitudinal reinforcement ratio can enhance the column's strength and stiffness, but it may also reduce its ductility. This is because a higher amount of longitudinal reinforcement can restrict the ability of the column to deform and elongate under load.

Additionally, changing the compressive strength of concrete from C25 to C50 can influence the ductility of the column. Both are under medium compressive strength of concrete. From the table 4.8, it can be observed that the ductility ratio of specimen reinforced with a stirrup with additional restraint plates slightly decreases as the compressive strength of concrete changed from C25 to C50. Higher strength concrete typically exhibits lower ductility compared to lower strength concrete. This is due to the fact that higher strength concrete tends to be more brittle and less capable of undergoing large deformations before failure.

Table 4. 8 Axial strain ductility ratio for the column

	Column label		ϵ_{85d}	ϵ_{cc}	u_{85d}
Group A	C25-SHA150	f_c' = 25mpa	5.76	2.86	2.01
	C25-SCTA150	ρ = 3.57%	8.07	3.02	2.67
	C25-SRPA150	S = 150mm	9.64	3.53	2.73
Group B	C25-SHB250	f_c' = 25mpa	9.08	3.14	2.89
	C25-SCTB250	ρ = 3.57%	7.26	2.90	2.50
	C25-SRPB250	S = 250mm	6.44	4.80	1.34
Group C	C25-SHC250	f_c' = 25mpa	5.10	2.86	1.78
	C25-SCTC150	ρ = 1.39%	8.85	2.99	2.96
	C25-SRPC150	S = 150mm	11.10	3.55	3.13
Group D	C25-SHD250	f_c' = 25mpa	5.56	3.07	1.81
	C25-SCTD250	ρ = 1.39 %	5.78	2.90	1.99
	C25-SRPD250	S = 250mm	5.32	2.70	1.97
Group E	C50-SHE150	f_c' = 50mpa	5.34	2.81	1.90
	C50-SCTE150	ρ = 3.57%	5.42	2.89	1.88
	C50-SRPE150	S = 150mm	7.11	2.85	2.49
Group F	C50-SHF250	f_c' = 50mpa	5.89	2.91	2.02
	C50-SCTF250	ρ = 3.57%	8.20	3.01	2.72
	C50-SRPF250	S = 250mm	5.25	2.84	1.85
Group G	C50-SHG150	f_c' = 50mpa	5.29	2.82	1.87
	C50-SCTG150	ρ = 1.39%	5.22	2.89	1.81
	C50-SRPG150	S = 150mm	6.48	2.85	2.27
Group H	C50-SHH250	f_c' = 50mpa	6.79	2.90	2.34
	C50-SCTH250	ρ = 1.39%	6.72	3.00	2.24
	C50-SRPH250	S = 250mm	4.53	2.67	1.70

4.2.7. Damage and Crack Pattern

The damage and crack behavior of the specimens was expressed in terms of concrete damage both in tension and compression, reinforcement Von Miss stress output and plastic strain of RC columns obtained from FEA simulations in ABAQUS Standard. The main indicator of cracking initiation in the concrete damage plasticity model is the value of maximum principal plastic strain. The concrete damaged plasticity (CDP) model states that concrete cracking begins as a result of positive maximum principal plastic strain (PE). Crack initiates when the maximum principal plastic strain is positive and the orientation of cracks is considered to be perpendicular to the maximum principal plastic strains, therefore in order to visualize the direction of cracking, the maximum principal plastic strain output is investigated [30]. Figure 4.8-4.13 illustrates the damage progress and developed crack patterns during the simulation.

a. Specimen C25-SHC150

The first tension damage and flexural cracks (maximum principal plastic strain) initiation was observed as shown in figure 4.8(a) and 4.9(a) at the top part of reinforced concrete column at the early stage of loading increment. During the early stage of loading increment, as the load is gradually applied to the column, tensile stresses start to develop at the top part of the column. These tensile stresses exceed the tensile strength of the concrete, leading to the initiation of tension damage and flexural cracks. When the full loading executed, the existing tensile damage and maximum principal plastic strain cracks continued to widen and extended as shown in specimen C25-SHC150. This is because the applied load further increases the tensile stresses in the concrete, causing the cracks to propagate. Figure 4.8 (b) and Figure 4.9(b) displays tensile damage and maximum principal plastic strain of the specimens respectively.

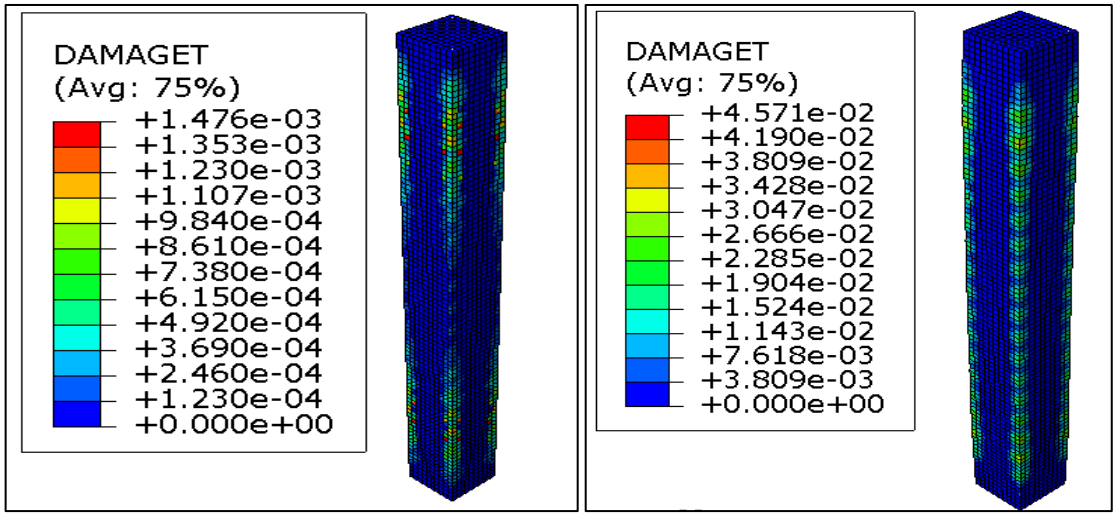

a b

Figure 4. 8: Concrete tensile damage of specimen C25-SHC150

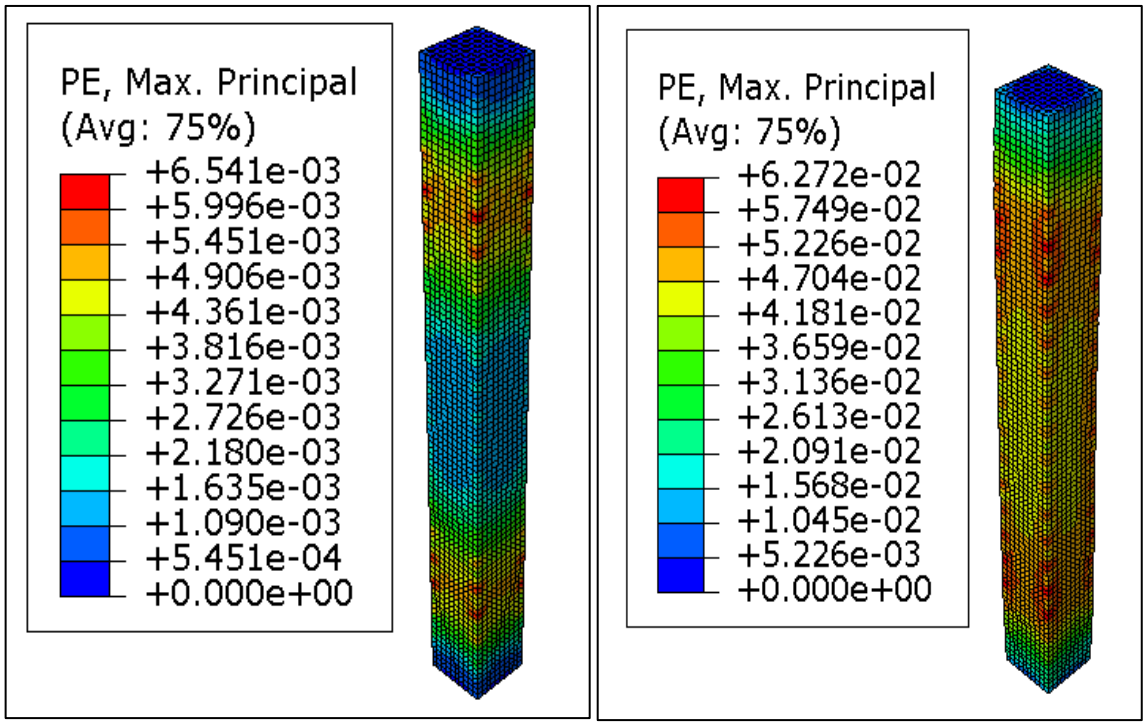

a. b.

Figure 4. 9: Maximum principal plastic strain of specimen C25-SHC150

b. Specimen C25-SCTC150

The first tension damage and flexural cracks (maximum principal plastic strain) initiation was observed as shown in figure 4.10(a) and 4.11(a) at the corner part of reinforced concrete column at the early stage of loading increment. when the full loading executed, the existing tensile damage and maximum principal plastic strain cracks continued to widen and extended as shown in specimen C25-SCTC150. Figure 4.10 (b)and Figure4.11(b) displays tensile damage and maximum principal plastic strain of the specimens respectively.

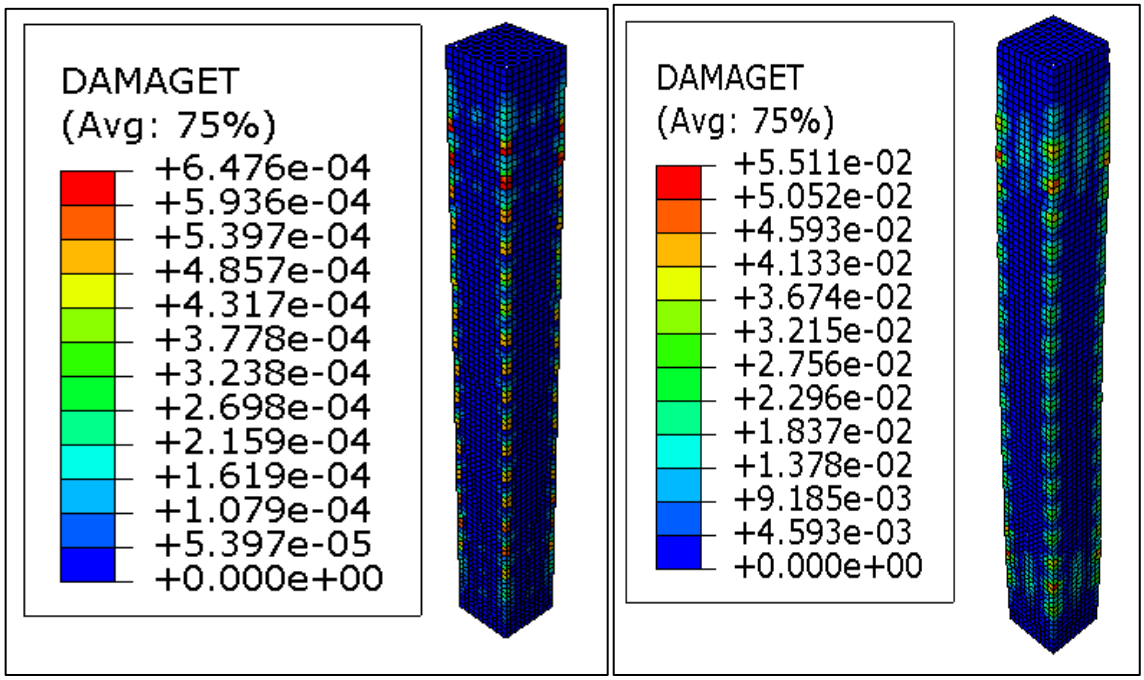

a b

Figure 4. 10: Concrete tensile damage of specimen C25-SCTC150

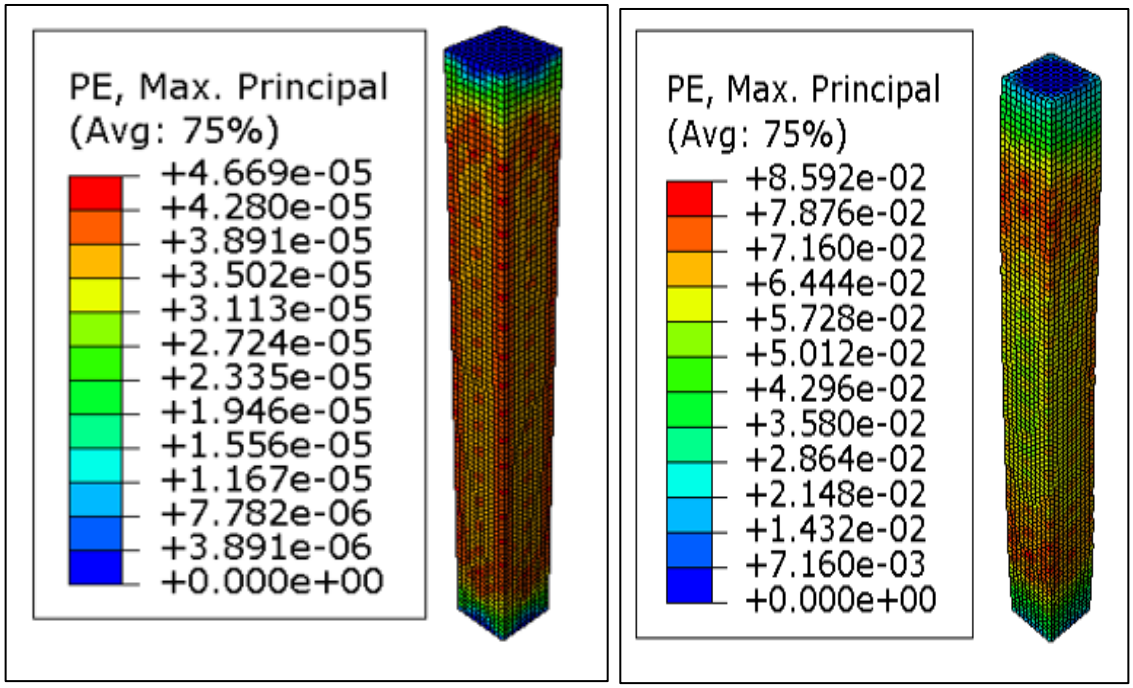

a. b.

Figure 4. 11: Maximum principal plastic strain of specimen C25-SCTC150

c. Specimen C25-SRPC150

The first tension damage and flexural cracks (maximum principal plastic strain) initiation was observed as shown in figure 4.12(a) and 4.13(a) at the middle part of reinforced concrete column where the restraint plate was located at the early stage of loading increment. when the full loading executed, the existing tensile damage and maximum principal plastic strain cracks continued to widen and extended as shown in specimen C25-SRPC150. Figure 4.12 (b) and Figure4.13(b) displays tensile damage and maximum principal plastic strain of the specimens respectively.

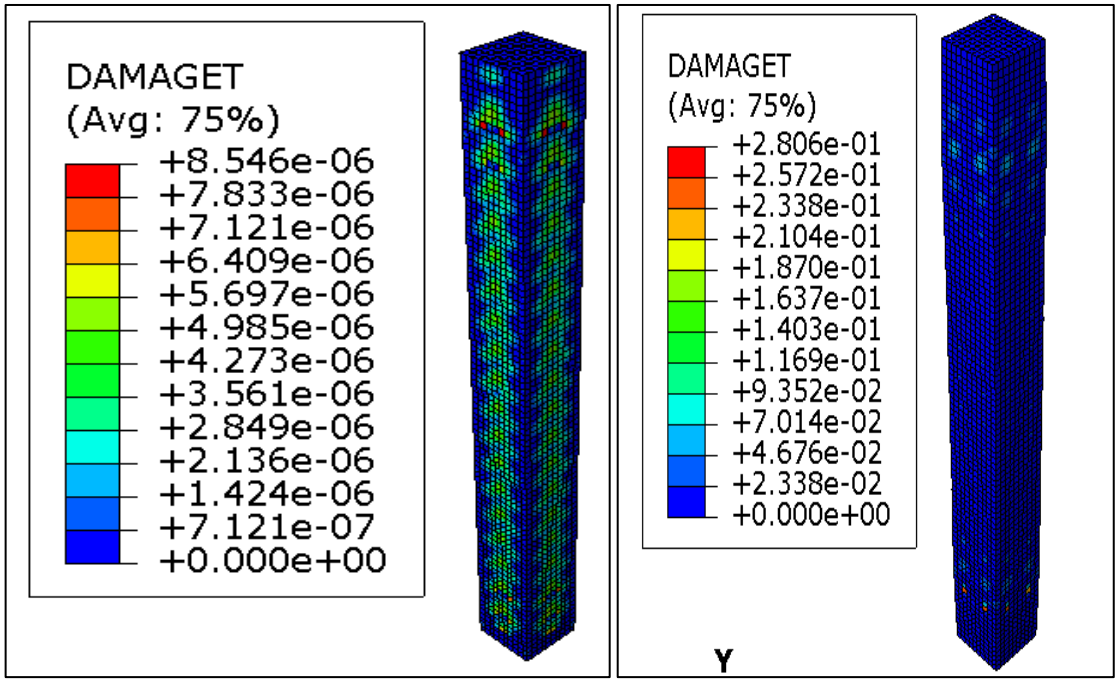

a. b.

Figure 4. 12: Concrete tensile damage of specimen C25-SRPC150

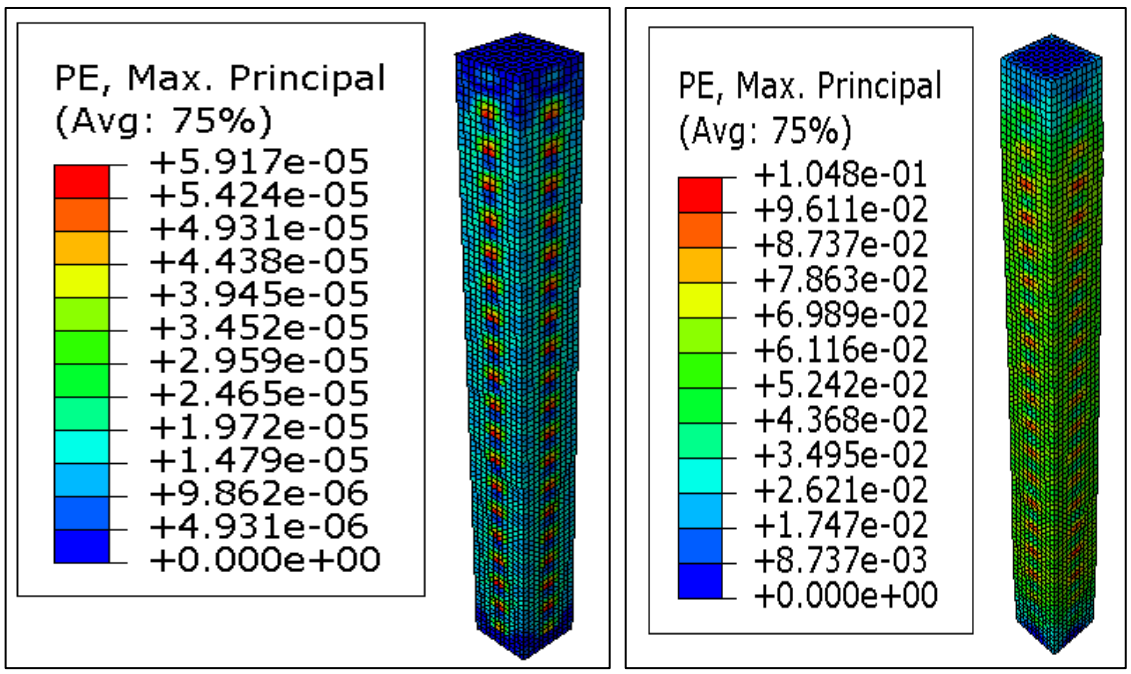

a. b.

Figure 4. 13: Maximum principal plastic strain of specimen C25-SRPC150

CHAPTER 5 CONCLUSIONS AND RECCOMENDATIONS

5.1 Conclusion

This study presented a consistent modeling methodology for reinforced concrete columns with different transverse reinforcement arrangements. It was based on a reliable three-dimensional nonlinear finite element method; concrete strengths, spacing of transverse reinforcement, transverse reinforcement configurations and influence of plate thickness were investigated under axial loading and the confinement action induced by a stirrup with additional restraint plates were identified. The structural behavior of the reinforced concrete column such as load-carrying capacity, ductility and modes of failure responses were predicted. Also, in this study, previous experimental study was validated by nonlinear finite element software.

According to finite element analysis result, the following findings were made,

- ✓ Results indicated that the three-dimensional finite element model used in this study was able to capture the major performance characteristics of reinforced concrete columns under axial loading by using ABAQUS/Explicit with the associated elements and material behavior models.
- ✓ The influence of concrete compressive strength and longitudinal reinforcement ratio significantly improves a column's strength and its ability to withstand axial loads. When concrete compressive strength increases from 25 MPa to 50 MPa, the ultimate load capacity of reinforced concrete columns increases by an average of 53%. While increasing longitudinal reinforcement ratio from 1.39% to 3.5% the ultimate load capacity of a reinforced concrete column increased by an average around 21% for C25 and 13 % for C50.
- ✓ The spacing of transverse reinforcement has a slight effect on the ultimate strength of reinforced concrete columns. When the spacing of transverse reinforcement increases from 150mm to 250mm there is an overall decrease in ductility ratio and decrease in column strength.
- ✓ The SRP configuration of transverse reinforcement improves a column's strength and its ability to withstand axial loads.

- ✓ The effect of plate thickness on the ultimate strength of reinforced concrete columns is almost negligible.

5.2 Recommendations

The following recommendations are made for future research:

The confinement effect caused by a particular type of stirrup with additional restraint plates on an axially loaded concrete column was the main topic of this paper. Future studies will look at how this new reinforcement scheme applies to more practical structural components, like actual-scale concrete beams and columns and beam-column joints subjected to cyclic loading.

The effectiveness of a reinforced concrete column was examined in this study using a small number of transverse reinforcement arrangements and parameters. Additional transverse reinforcement arrangements, such as circular sections with cross ties and others, will be studied in future studies to examine the performance of reinforced concrete columns.

REFERENCES

[1] Tedros Kiros, (2018). Experimental and Analytical Investigation on Spiral and Circular Hoop Confinement of Concrete. MSc. Thesis, Addis Ababa University, Addis Ababa, Ethiopia.

[2] Sheikh, S.A. (1978). Effectiveness of rectangular ties as confinement steel in reinforced concrete columns. PhD dissertation, Department of Civil Engineering, University of Toronto, Canada.

[3] Mourad, S.M. and Shannag, M.J. (2012). Repair and strengthening of reinforced concrete square Columns using ferrocement jackets. Cement and Concrete Composite, vol.34, no.2, pp. 288–294.

[4] Kumar, P.R., Oshima, T. and Mikami, S. (2004). Ferrocement confinement of plain and reinforced concrete. Program Structural Engineering Material, vol.6, no.4, pp. 241–51.

[5] Saatcioglu, M. and Grira, M. (1999). Confinement of reinforced concrete columns with welded reinforcement girds. ACI Structural journal, vol.96, no.1, pp.29–39.

[6] Ksuma, B., Tavio and Suprobo, P. (2011). Axial load behavior of concrete columns with welded wire fabric as transverse reinforcement. Procedia Engineering journal, vol.14, pp.2039–2047.

[7] Eseteselase Berhanu, (2020). Confinement Effect of Structural Steel and Transverse Reinforcement on Axial Compression Resistance of Concrete Encased Composite Column. MSc. Thesis, Addis Ababa University, Addis Ababa, Ethiopia.

[8] Ahmed, A.R.and Hayder, R. (2016). Combined Transverse Steel-External FRP Confinement Model for Rectangular Reinforced Concrete Columns.

[9] Mander, J.B., Priestley, M.J.N. and Park, R. (1988). Theoretical Stress-Strain Model for Confined Concrete. Journal of Structural Engineering, ASCE, vol. 114, no.8, pp. 1804-1826.

[10] Elwood, K.J. and Eberhard, M.O. (2009). Effective stiffness of reinforced concrete columns. ACI Structural Journal, vol. 106, no.4, pp. 476- 484.

[11] Shafqat, A. and Ali, A. (2012). Lateral Confinement of RC Short Column. Sci. Int. (Lahore), vol.24, no.4, pp. 371-379.

[12] Melat Ayele. (2010). Experimental and Analytical Investigation on Confined Reinforced Concrete Column. MSc. Thesis, Addis Ababa University, Addis Ababa, Ethiopia.

[13] Sotoud, S. and Aboutaha, R. S. (2014). Performance of RC Bridge Columns Subjected to Lateral Loading, Istanbul Bridge Conference. Proceedings of the Istanbul Bridge Conference, Istanbul, Turkey.

[14] Ahmed, M.K. and Hany, A.D. (2016). Improved confinement of reinforced concrete column. Ain Shams Engineering Journal, pp.717-728.

[15] Paulay, T. and Priestley, M.J.N. (1992). Seismic Design of Reinforced Concrete and Masonry Buildings. John Wiley and Sons, New York.

[16] Kent, D. C. and Park, R. (1971). Flexural members with confined concrete. Journal of the Structural Division, Proceedings, ASCE, vol.97, no.ST7.

[17] Roy, E. H., and Sozen, M. A. (1967). Ductility of concrete. Journal of the Structural Division, vol.93, no.3, pp. 107-144.

[18] Soliman, M. Y. and Yu, T. X. (1997). Ductility of reinforced concrete beams. Journal of Structural Engineering, vol.123, no.4, pp. 449-456.

[19] Scott, B. D., Park, R. and Priestley, M. J. N. (1982). Stress-strain behavior of concrete confined by overlapping hoops at low and high strain rates. American Concrete Institute, vol.79, pp. 13-27.

[20] Popovics, S. A. (1973). Numerical Approach to the Complete Stress-Strain Curve of Concrete. Cement and Concrete Research, vol.3, no.5, pp. 583–599.

[21] William, K. J. and Warnke, E. P. (1975). Constitutive model for the triaxial behavior of concrete. Proceedings, International Association for Bridge and Structural Engineering, vol. 19, pp. 1-30.

[22] Li, B., Park, R. and Tanaka, H. (2001). Stress-strain behavior of high-strength concrete confined by ultra-high and normal-strength transverse reinforcements. ACI Structural Journal, vol. 98, no.3, pp. 395-406.

[23] Dario, D. D., Devid, F. and Giuseppe, R. (2019). Confinement effect of different arrangements of transverse reinforcement on axially loaded concrete columns: An experimental study. Journal of the Mechanical Behavior of Materials, vol. 28 pp.13–19.

[24] Mahmoud, F. B., Hatem, M. M. and sheriff, A. M. (2014). Behavior of reinforced concrete columns strengthened by steel jacket. Housing and Building National Research Center journal.

[25] Syed, W. N. R., Shaikh, M.G. (2018). Effect of confinement on behavior of short concrete column. Procedia Manufacturing, vol.20, pp. 563 – 570.

[26] Kim, J.K. and Park, C.K. (1999). The Behavior of Concrete Columns with Interlocking Spirals. Engineering Structure, vol.21, pp. 945–953.

[27] Mariateresa, G., Alfonso, D., Anna, T. and Giuseppe, F. (2020). Experimental Behavior of Concrete Columns Confined by Transverse Reinforcement with Different Details.

[28] ABAQUS (2017). Theory Manual, and User Manual Version 2017.Dassault Systems Simulia Corp, Providence, RI.

[29] Jankowiak, T. and Lodygowski, T. (2005). Identification of parameters of concrete damage plasticity constitutive model. Foundations of Civil and Environmental Engineering, vol. 6, no.5, pp. 960–975.

[30] M.A. Najafgholipour, S.M. Dehghan, Amin D. and Arsalan, N. (2017). Finite Element Analysis of Reinforced Concrete Beam-Column Connections with Governing Joint Shear Failure Mode. Latin American Journal of solids and structures, vol. 14, no.7, pp. 1200 – 1225.

[31] Lee, J. and Fenves, G.L. (1998). Plastic-Damage Model for cyclic loading of concrete structures. Journal of Engineering Mechanics. Vol.124, no.8, pp. 892-900.

[32] Wu, J.Y., Li, J. and Faria, R. (2006). An energy release rate-based plastic-damage model for concrete, International Journal of Solids and Structures, vol. 43, no.3, pp.583–612.

[33] Voyiadjis, G.Z. and Taqieddin, Z.N. (2009). Elastic plastic and damage model for concrete materials: Part I – Theoretical formulation. International Journal Structure Changes Solids, vol.1, no.1, pp.31–59.

[34] Xiang, Z. (2017). Finite Element Analysis of Square RC Columns Confined by Different Configurations of Transverse Reinforcement. Civil Engineering Journal, vol.11, pp. 292-302.

[35] Ren, W., Sneed, L., Yang, Y. and He, R. (2014). Numerical Simulation of Prestressed Precast Concrete Bridge Deck Panels Using Damage Plasticity Model. International Journal of Concrete Structures and Materials, pp. 2234-1315.

[36] Behnam, H., Kuang, J. S. and Samali, B. (2018). Parametric finite element analysis of RC wide beam-column connections, Computers and Structures.

[37] Cusson and Paultre, P. (1994). High-strength concrete columns confined by rectangular ties, Journal of Structural Engineering, ASCE, vol.120, no.3, pp.783–804.

[38] Murat Saatcioglu, (1992). Strength and Ductility of Confined Concrete. Journal of structural Engineering.

[39] Karabinis, A. I. and Kiousis, P. D. (1996). Strength and Ductility of Rectangular Concrete Columns: A Plasticity Approach. Journal of Structural Engineering, ASCE, vol. 122, no. 3, pp. 267-274.

[40] Shanan, M. A., Elzanaty A.and Metwally K. (2016). Effect of Concrete Strength and Aspect Ratio on Strength and Ductility of Concrete Columns. International Journal of Civil, Environment, Structural, Construction and Architectural Engineering vol.10, no.7.

APPENDIX A

A.1 Material Property with Damage Parameter of Concrete Used for parametric study

The concrete and steel reinforcement material properties that is used in in the reinforced concrete column simulations are given in table A.1.1 and A.1.2 respectively. In this study, two types of concrete compressive strength were used for simulation.

Table A.1.1: Material property for grade C-25 concrete with damage parameter of concrete for parametric study

Compression Behavior		Compression Damage	
Yield stress (MPa)	Inelastic strain	Damage Parameter	Inelastic strain
12.71311475	0	0	0
16.45864662	0.000246	0	0.0002457
19.91747573	0.000331	0	0.0003305
23.06024096	0.000427	0	0.0004267
25.85343035	0.000535	0	0.0005353
28.25862069	0.000658	0	0.0006577
30.23154362	0.000796	0	0.0007956
31.72093023	0.000951	0	0.0009508
32.66707022	0.001125	0	0.0011253
33	0.001322	0	0.0013218
32.96649494	0.001387	0.0010153	0.0013873
32.86415612	0.001455	0.0041165	0.0014552
32.69013486	0.001526	0.0093899	0.0015257
32.44142309	0.001599	0.0169266	0.0015989
32.11484204	0.001675	0.026823	0.0016748
31.70702999	0.001754	0.0391809	0.0017537
31.21442886	0.001836	0.0541082	0.0018355
30.63326969	0.001921	0.0717191	0.0019206
29.95955681	0.002009	0.0921346	0.0020089
29.18905047	0.002101	0.1154833	0.0021007
28.31724797	0.002196	0.1419016	0.0021961
27.33936292	0.002295	0.1715345	0.0022953
26.25030257	0.002398	0.2045363	0.0023985
25.04464286	0.002506	0.2410714	0.0025058

Tension Behavior		Tension Damage	
Yield stress (MPa)	Inelastic strain	Damage Parameter	Inelastic strain
3.092264	0	0	0
2.886113	0.003691	0.066667	0.003691
2.679962	0.007383	0.133333	0.007383
2.473811	0.011074	0.2	0.011074
2.26766	0.014766	0.266667	0.014766
2.061509	0.018457	0.333333	0.018457
1.855358	0.022149	0.4	0.022149
1.649207	0.02584	0.466667	0.02584
1.443056	0.029532	0.533333	0.029532
1.236906	0.033223	0.6	0.033223
1.030755	0.036915	0.666667	0.036915
0.824604	0.040606	0.733333	0.040606
0.618453	0.044297	0.8	0.044297
0.58753	0.053157	0.81	0.053157
0.555963	0.062201	0.820208	0.062201
0.524396	0.071245	0.830417	0.071245
0.49283	0.080289	0.840625	0.080289
0.461263	0.089333	0.850833	0.089333
0.429696	0.098377	0.861042	0.098377
0.398129	0.107421	0.87125	0.107421
0.366562	0.116465	0.881458	0.116465
0.334995	0.125509	0.891667	0.125509
0.303428	0.134554	0.901875	0.134554
0.271862	0.143598	0.912083	0.143598
0.240295	0.152642	0.922292	0.152642
0.208728	0.161686	0.9325	0.161686
0.177161	0.17073	0.942708	0.17073
0.145594	0.179774	0.952917	0.179774

Table A.1.2: Material property for grade C-50 concrete with damage parameter of concrete for parametric study

Compression Behavior		Compression Damage	
Yield stress (MPa)	Inelastic strain	Damage Parameter	Inelastic strain
22.3442623	0	0	0
28.9273183	2.96915E-05	0	2.96915E-05
35.0064725	6.91373E-05	0	6.91373E-05
40.5301205	0.000124016	0	0.000124016
45.4393624	0.000195964	0	0.000195964
49.6666667	0.000286856	0	0.000286856
53.1342282	0.000398856	0	0.000398856
55.751938	0.000534466	0	0.000534466
57.4148507	0.000696601	0	0.000696601
58	0.000888678	0	0.000888678
57.9411123	0.0009546	0.001015305	0.0009546
57.7612441	0.001023882	0.004116481	0.001023882
57.4553885	0.001096665	0.009389853	0.001096665
57.0182588	0.001173095	0.016926573	0.001173095
56.4442678	0.001253327	0.026822968	0.001253327
55.7275073	0.001337525	0.039180909	0.001337525
54.8617234	0.001425864	0.054108216	0.001425864
53.8402922	0.001518526	0.0717191	0.001518526
52.6561908	0.001615708	0.092134642	0.001615708
51.3019675	0.001717616	0.115483319	0.001717616
49.7697086	0.00182447	0.141901577	0.00182447
48.0510015	0.001936504	0.171534457	0.001936504
46.1368954	0.002053966	0.204536286	0.002053966
44.0178571	0.002177122	0.241071429	0.002177122

Tension Behavior		Tension Damage	
Yield stress (MPa)	Inelastic strain	Damage Parameter	Inelastic strain
4.063876	0	0	0
3.792951	0.003109	0.066667	0.003109
3.522026	0.006218	0.133333	0.006218
3.251101	0.009327	0.2	0.009327
2.980176	0.012436	0.266667	0.012436
2.709251	0.015545	0.333333	0.015545
2.438326	0.018654	0.4	0.018654
2.167401	0.021763	0.466667	0.021763
1.896475	0.024872	0.533333	0.024872
1.62555	0.027981	0.6	0.027981
1.354625	0.03109	0.666667	0.03109
1.0837	0.034199	0.733333	0.034199
0.812775	0.037308	0.8	0.037308
0.772136	0.044769	0.81	0.044769
0.730651	0.052386	0.820208	0.052386
0.689166	0.060003	0.830417	0.060003
0.64768	0.06762	0.840625	0.06762
0.606195	0.075237	0.850833	0.075237
0.564709	0.082854	0.861042	0.082854
0.523224	0.090471	0.87125	0.090471
0.481739	0.098088	0.881458	0.098088
0.440253	0.105705	0.891667	0.105705
0.398768	0.113322	0.901875	0.113322
0.357282	0.120939	0.912083	0.120939
0.315797	0.128556	0.922292	0.128556
0.274312	0.136173	0.9325	0.136173
0.232826	0.14379	0.942708	0.14379
0.191341	0.151407	0.952917	0.151407

APPENDIX B

Reinforcement Mises Stress

i. Specimens under Group A

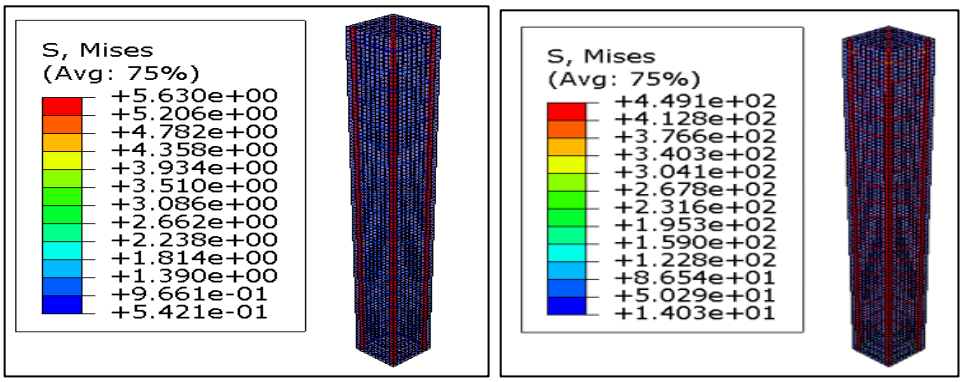

a. C25 – SHA150

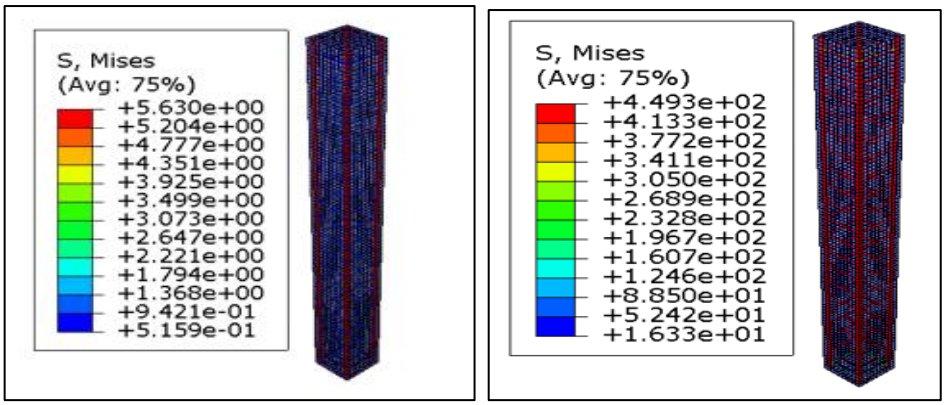

b. C25 – SCTA150

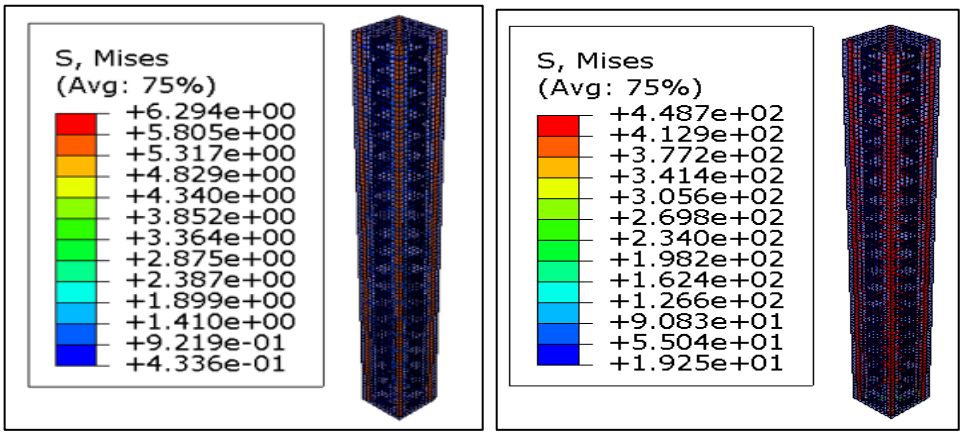

c. C25 – SRPA150

ii. Specimens under Group B

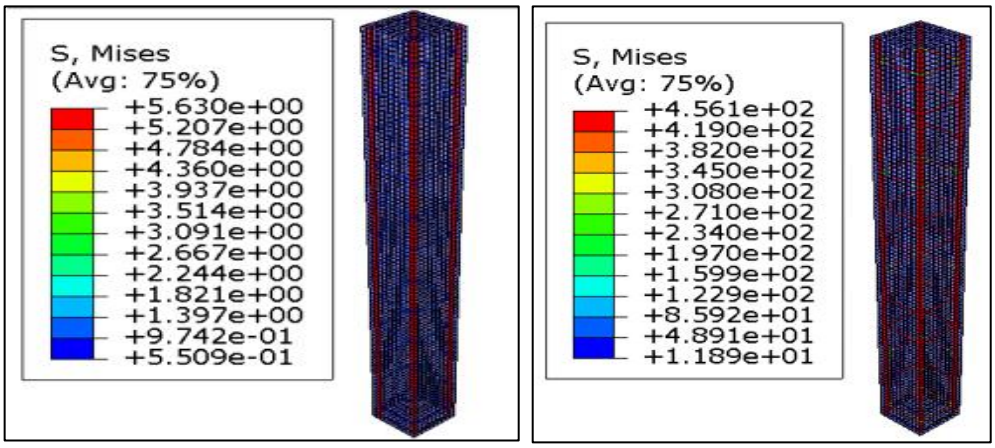

a. C25 – SHB250

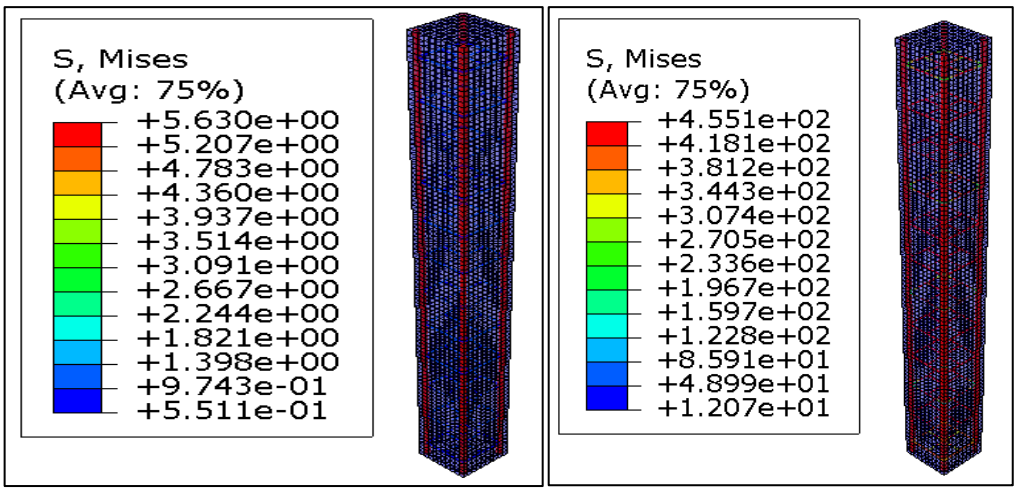

b. C25 – SCTB250

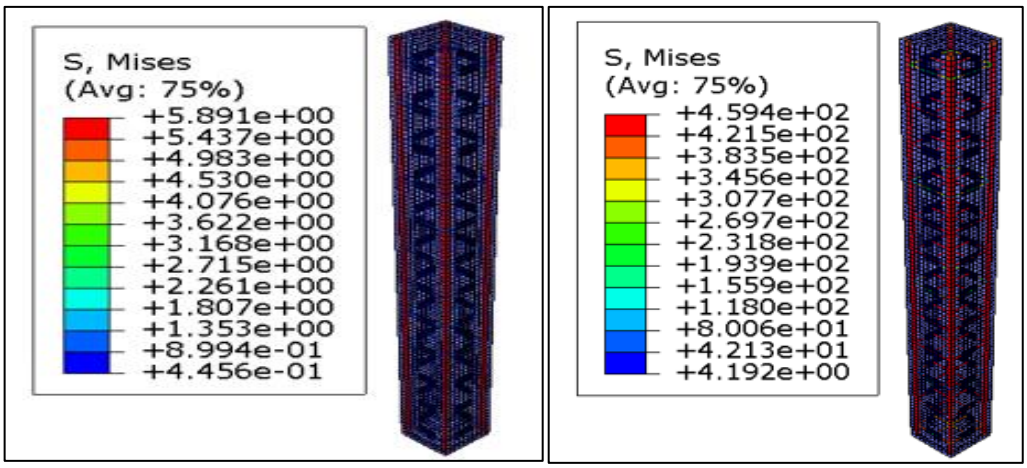

c. C25 – SRPB250

iii. Specimens under Group C

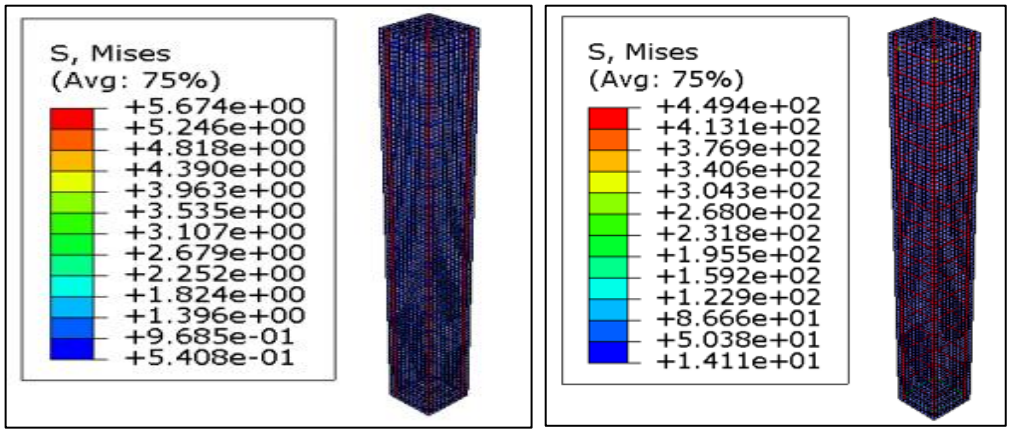

a. C25 – SHC150

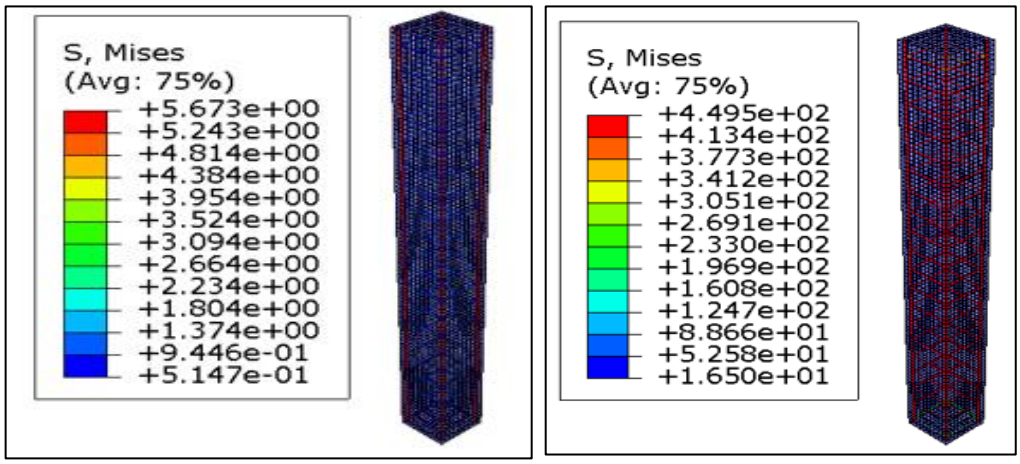

b. C25 – SCTC150

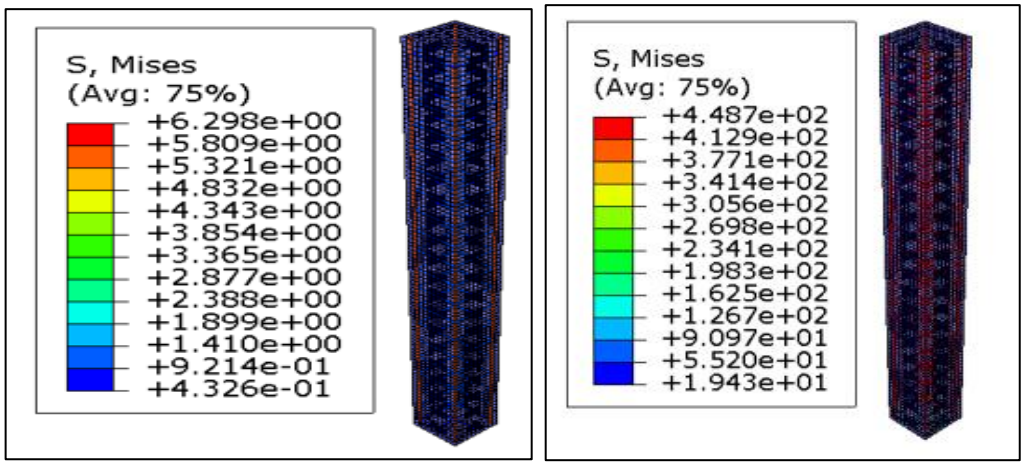

c. C25 – SRPC150

iv. Specimens under Group E

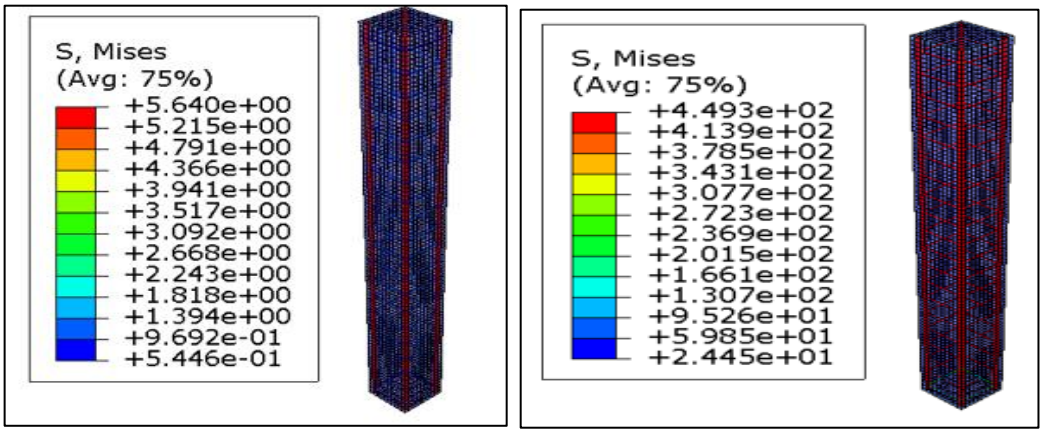

a. C50 – SHE150

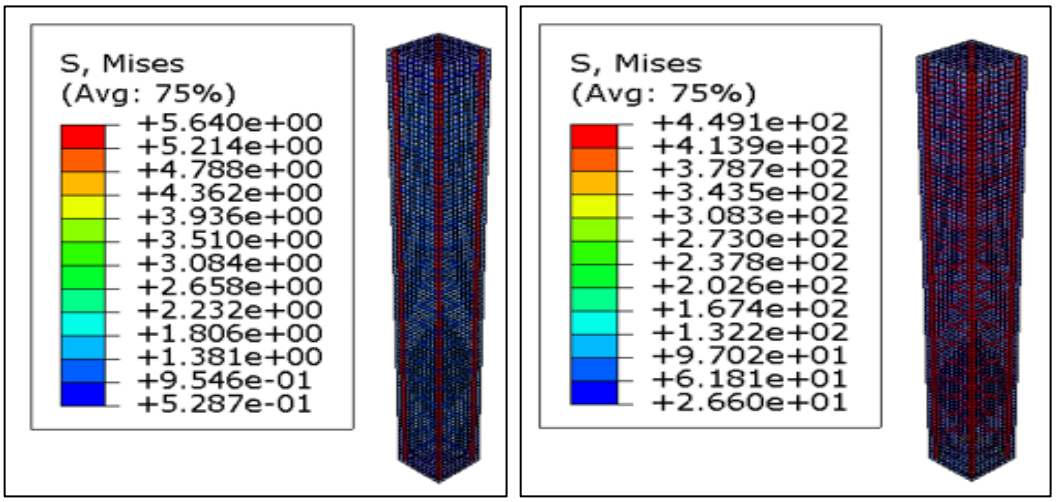

b. C50 – SCTE150

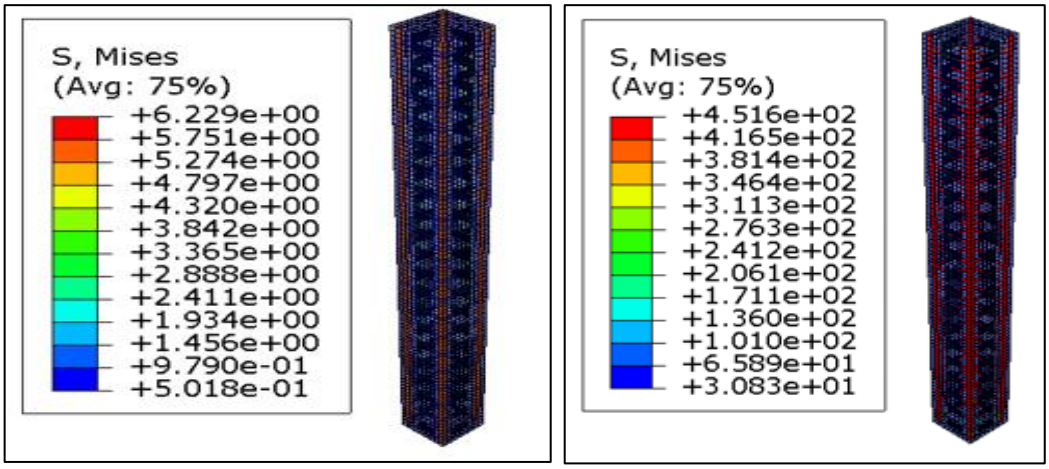

c. C50 – SRPE150